Magmatic and tectonic evolution of the Caetano caldera, north-central Nevada: A tilted, mid-Tertiary eruptive center and source of the Caetano Tuff

David A. John
U.S. Geological Survey, 345 Middlefield Road, Menlo Park, California 94025, USA

Christopher D. Henry
Nevada Bureau of Mines and Geology, University of Nevada, Reno, Nevada 89557, USA

Joseph P. Colgan
U.S. Geological Survey, 345 Middlefield Road, Menlo Park, California 94025, USA

ABSTRACT

The Caetano Tuff is a late Eocene, rhyolite ash-flow tuff that crops out within an ~90-km-long, east-west–trending belt in north-central Nevada, previously interpreted as an elongate graben or "volcano-tectonic trough." New field, petrographic, geochemical, and geochronologic data show that: (1) the east half of the "trough" is actually the Caetano caldera, formed by eruption of the Caetano Tuff at 33.8 Ma and later structurally dismembered during Miocene extension; (2) the west half of the trough includes both the distinctly younger and unrelated Fish Creek Mountains caldera (ca. 24.7 Ma) and a west-trending paleovalley partly filled with outflow Caetano Tuff; and (3) the Caetano Tuff as previously defined actually consists of three distinct units, two units of the 33.8 Ma Caetano Tuff and an older (34.2 Ma) tuff, exposed north of the Caetano caldera, herein named the tuff of Cove Mine.

Miocene extensional faulting and tilting has exposed the Caetano caldera over a paleodepth range of >5 km, from the caldera floor through post-caldera sedimentary rocks, providing exceptional constraints on an evolutionary model of the caldera that are rarely available for other calderas. The Caetano caldera filled with more than 4 km of intracaldera Caetano Tuff, while outflow tuff flowed west and south of the caldera, primarily down Eocene paleovalleys. Caldera fill consists of two units of Caetano Tuff. The lower compound cooling unit is as much as 3600 m thick and is separated by a complete cooling break from a 500–1000-m-thick upper unit that consists of multiple, thin, ash flows interbedded with sedimentary deposits. Multiple granite porphyries, including the 25-km^2 Carico Lake pluton, intruded and domed the center of the caldera within 0.1 Ma of caldera formation; one of these porphyries is associated with pervasive argillic and advanced argillic alteration of the western half of the caldera. All exposed caldera-related rocks are rhyolites or granites (71–77.5 wt% SiO_2). Caldera collapse was significantly greater than the thickness of caldera fill and created a topographic depression that served as a depocenter until at least 25 Ma, filling with nearly 1 km of sediments and distally derived, ash-flow tuffs.

The caldera is presently exposed in a series of 40–50°, east-tilted blocks bounded by north-striking, west-dipping normal faults that formed after 16 Ma. Slip on these faults accommodated ~100% E-W extension, making the restored Caetano caldera ~20 km east-west by 10–18 km north-south. The estimated volume of intracaldera Caetano Tuff is, therefore, ~840 km^3, and the minimum estimated total eruptive volume is ~1100 km^3. Although the Caetano magmatic system was probably too young to supply heat for nearby Carlin-type gold deposits in the Cortez district, earlier nearby magmatic activity may have contributed to formation of these deposits. Reconstruction of the late Eocene, pre-Caetano caldera geologic setting, immediately prior to caldera formation, indicates that the Cortez Hills and Horse Canyon Carlin-type deposits formed at ≤1 km depths.

Keywords: calderas, ash-flow tuff, magma resurgence, Basin and Range Province, extensional tectonics, Carlin-type gold deposit.

INTRODUCTION

The Caetano Tuff in north-central Nevada is one of the volumetrically largest manifestations of vigorous mid-Tertiary (ca. 43–19 Ma) magmatism dominated by voluminous caldera-forming ash flow eruptions (Lipman et al., 1972; Best et al., 1989; Christiansen and Yeats, 1992). Carlin-type gold deposits in northern Nevada, which are among the largest gold deposits in the world and help make Nevada the second largest gold producer in the world (Price and Meeuwig, 2006), formed during this magmatism between 42 and 30 Ma (Hofstra et al., 1999; Fig. 1). Widespread tuffs that issued from the calderas can be dated with great precision, and, together with younger volcanic and sedimentary rocks, they provide key markers for determining the timing and magnitude of magmatism and extension relative to the formation of Carlin-type gold deposits (e.g., Cline et al., 2005). The Caetano Tuff is a regionally widespread, late Eocene, ash-flow tuff in north-central Nevada (Fig. 1; Masursky, 1960; Gilluly and Masursky, 1965; Stewart and McKee, 1977). It is the only extensive, mid-Tertiary volcanic unit between the Tuscarora Mountains, ~120 km to the north of exposures of the Caetano Tuff (Castor et al., 2003; Henry, 2008), and the vast expanse of Oligocene and Miocene calderas >75 km to the south (Fig. 1; Best et al., 1989; Ludington et al., 1996). The Caetano Tuff and related rocks thus offer one of the few windows into the history of Cenozoic magmatism, extension, and ore deposit formation in the adjacent Battle Mountain-Eureka trend, which boasts several world-class, Carlin-type gold deposits.

The Caetano Tuff mostly occupies a west-trending belt ~40 km long by 10–18 km wide

Geosphere; February 2008; v. 4; no. 1; p. 75–106; doi: 10.1130/GES00116.1; 20 figures; 1 plate, 2 tables, 3 appendices.

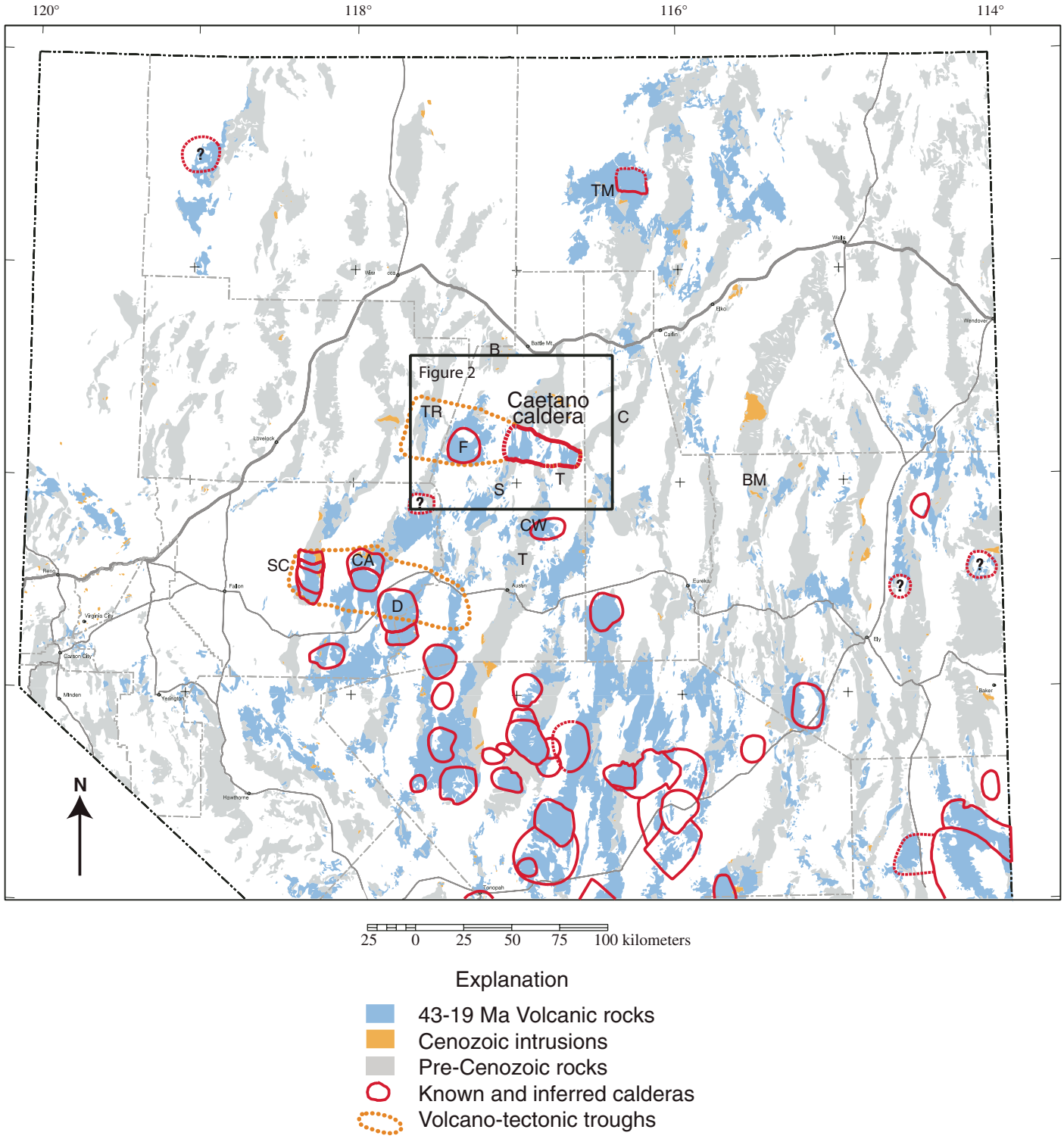

Figure 1. Map showing mid-Cenozoic (43–19 Ma) volcanic rocks and intrusions in northern Nevada and calderas (modified from Ludington et al. [1996]) and volcano-tectonic troughs of Burke and McKee (1979). Box shows outline of Figure 2. B—Battle Mountain; BM—Bald Mountain; C—Cortez Range; CA—Clan Alpine Range calderas; CW—Cowboys Rest; D—Desatoya Mountains calderas; F—Fish Creek Mountains caldera; S—Shoshone Range; SC—Stillwater caldera complex; T—Toiyabe Range; TM—Tuscarora volcanic field; TR—Tobin Range.

that has been described as the eastern half of a fault-bounded, volcano-tectonic trough (Masursky, 1960). As originally defined, the trough was inferred to extend ~90 km west from Grass Valley on the west side of the Cortez Range to Pleasant Valley on the west side of the Tobin Range (Figs. 1 and 2; Burke and McKee, 1979). This inferred structural control on the distribution of the tuff implied a late Eocene to early Oligocene episode of north-south extension not recognized elsewhere in the northern Great Basin. We interpret these relations as two middle-Tertiary calderas modified by Miocene Basin and Range extension. The thickest exposures(>3.4 km) of the Caetano Tuff are in the northern Toiyabe Range a few kilometers southwest of the Cortez and Cortez Hills Carlin-type gold deposits and ~10 km south of the Pipeline and Gold Acres Carlin-type gold deposits (Fig. 2). Rhyolite dikes of similar composition but slightly older age than the Caetano Tuff are exposed in the Cortez Mine, where they have been variably interpreted to both pre-date and post-date formation of Carlin-type ores (Wells et al., 1969; Rytuba, 1985; McCormack and Hays, 1996; Mortensen et al., 2000).

New field, petrographic, geochemical, and geochronologic data for the Caetano Tuff and related intrusive rocks are presented in this paper and in a companion paper (Colgan et al., 2008) that bear on the origin and source of the Caetano Tuff and the tectonic evolution of the surrounding area, including post-ore (<34 Ma) deformation of major nearby Carlin-type gold deposits. We have remapped the caldera, including caldera margins, the caldera floor, resurgent intrusions, and intracaldera stratigraphy (Plate 1). These data show that tuffs previously correlated with Caetano Tuff consist of two distinct, ash-flow tuff units erupted ca. 400 ka apart: (1) the tuff of Cove Mine, a slightly older and more mafic outflow tuff that mostly crops out north of the Caetano caldera and erupted from an unidentified source, and (2) multiple cooling units of Caetano Tuff that fill the highly extended, structurally dismembered Caetano caldera and flowed primarily south and west of the caldera (Fig. 2). Reconstruction of the Caetano caldera provides a strain marker for constraining later extension, and the companion paper (Colgan et al., 2008) uses the reconstructed caldera to document Late Cenozoic extension and the regional implications of this extension on adjacent Carlin-type gold deposits.

METHODS OF STUDY

Major objectives of this study included (1) distinguishing between caldera versus volcano-tectonic trough origins for the "Caetano trough"; (2) in the case of a caldera origin, determining the timing and duration of ash-flow eruption, caldera collapse, and resurgent doming; (3) determining whether previously mapped "Caetano Tuff" (including intracaldera and outflow tuff) is all the same tuff; and (4) constraining the timing of post-caldera events, including the timing of major E-W extension. To accomplish these objectives, we compiled a 1:100,000-scale geologic map of the caldera (Plate 1), based on new geologic mapping of key localities at 1:24,000 scale, and we conducted petrographic, geochemical, and geochronologic analyses of samples collected throughout the caldera and surrounding region (Fig. 2; Appendices 1A, 1B, and 2[1]).

To aid in correlation of the widely distributed tuffs, ~100 thin sections of previously mapped Caetano Tuff and related intrusive rocks were examined petrographically, and modal analyses were made for ~75 samples. Modally analyzed samples were divided into groups of intracaldera Caetano Tuff, extracaldera Caetano Tuff, intrusive rocks, and the tuff of Cove Mine as described in the next section.

Seventy-two whole-rock samples of the Caetano Tuff, tuff of Cove Mine, and intrusive rocks in Carico Lake Valley were analyzed for major and trace elements by XRF (X-ray fluorescence) techniques (Appendix 1A and 1B). Most tuff samples were devitrified and densely welded, and we did not try to separate the strongly flattened, crystal-rich pumice blobs. Our new chemical analyses were combined with ~25 previously published analyses in Roberts (1964), Gilluly and Masursky (1965), Stewart and McKee (1977), Doebrich (1995), Gonsior (2006), and M.G. Best (2004, written commun.). About 20% of all analyzed samples were strongly hydrothermally altered, as indicated by the presence of hydrothermal minerals (e.g., calcite or kaolinite) or by high SiO_2 or K_2O and/or low Na_2O contents; these analyses were discarded. The remaining, relatively unaltered samples were divided into groups of intracaldera Caetano Tuff, extracaldera Caetano Tuff, intrusive rocks, and the tuff of Cove Mine using the same divisions as for the modal data.

Published K-Ar dates from the Caetano Tuff range from 31.3 ± 0.6 to 35.3 ± 1.1 Ma (Sloan et al., 2003) and are insufficiently precise to address major objectives of this study. Single crystal $^{40}Ar/^{39}Ar$ dating of sanidine provides highly precise, reproducible ages that can distinguish volcanic events separated by as little as 100,000 yr at the ca. 34 Ma age of the Caetano Tuff(s) (Deino, 1989; McIntosh et al., 1990; Henry et al., 1997). Therefore, we determined 15 new, sanidine, single-crystal $^{40}Ar/^{39}Ar$ ages for previously mapped Caetano Tuff and a related pluton (Table 1). We also determined $^{40}Ar/^{39}Ar$ ages for intracaldera Fish Creek Mountains Tuff 15 km west of the Caetano caldera (Fig. 2) and for a tuff that resembles the Caetano Tuff from Bald Mountain 100 km to the east (Fig. 1). Analytical techniques and data are provided in Appendix 2.

GEOLOGY OF THE CAETANO CALDERA

Due to large magnitude (~100%) east-west extension along west-dipping normal faults in the middle Miocene (Colgan et al., 2008), the Caetano caldera is exceptionally well exposed in a series of east-tilted fault blocks. The entire stratigraphy of the caldera fill is exposed (Fig. 3), as well as a wide range of pre- and post-caldera rocks, thereby allowing a more complete understanding of caldera evolution than seen in most calderas. Numerous caldera-related structural features are evident, including the caldera floor and margins, mesobreccias and megabreccias, resurgent intrusions, and post-collapse, caldera-filling sediments. This section emphasizes caldera-related rocks but also briefly summarizes pre- and post-caldera rocks. Detailed field descriptions of caldera stratigraphy, structure, and hydrothermal features are presented in subsequent sections.

Pre-Cenozoic Basement Rocks

Complexly deformed Paleozoic sedimentary rocks form the basement beneath the Caetano caldera. Lower Paleozoic siliciclastic rocks of the upper plate of the Roberts Mountains allochthon probably underlie most of the caldera. These rocks structurally overlie lower plate Neoproterozoic-Devonian, carbonate-rich, continental-shelf sedimentary rocks. The two sequences were superimposed along the Roberts Mountains thrust during the Late Devonian-Early Mississippian Antler orogeny (Roberts et al., 1958). The Roberts Mountains allochthon is overlain unconformably by Pennsylvanian-Permian clastic and

[1]If you are viewing the PDF of this paper or reading it offline, please visit http://dx.doi.org/10.1130/GES00116.S1, http://dx.doi.org/10.1130/GES00116.S2, and http://dx.doi.org/10.1130/GES00116.S3 or the full-text article on www.gsajournals.org to access Appendices 1A, 1B, and 2.

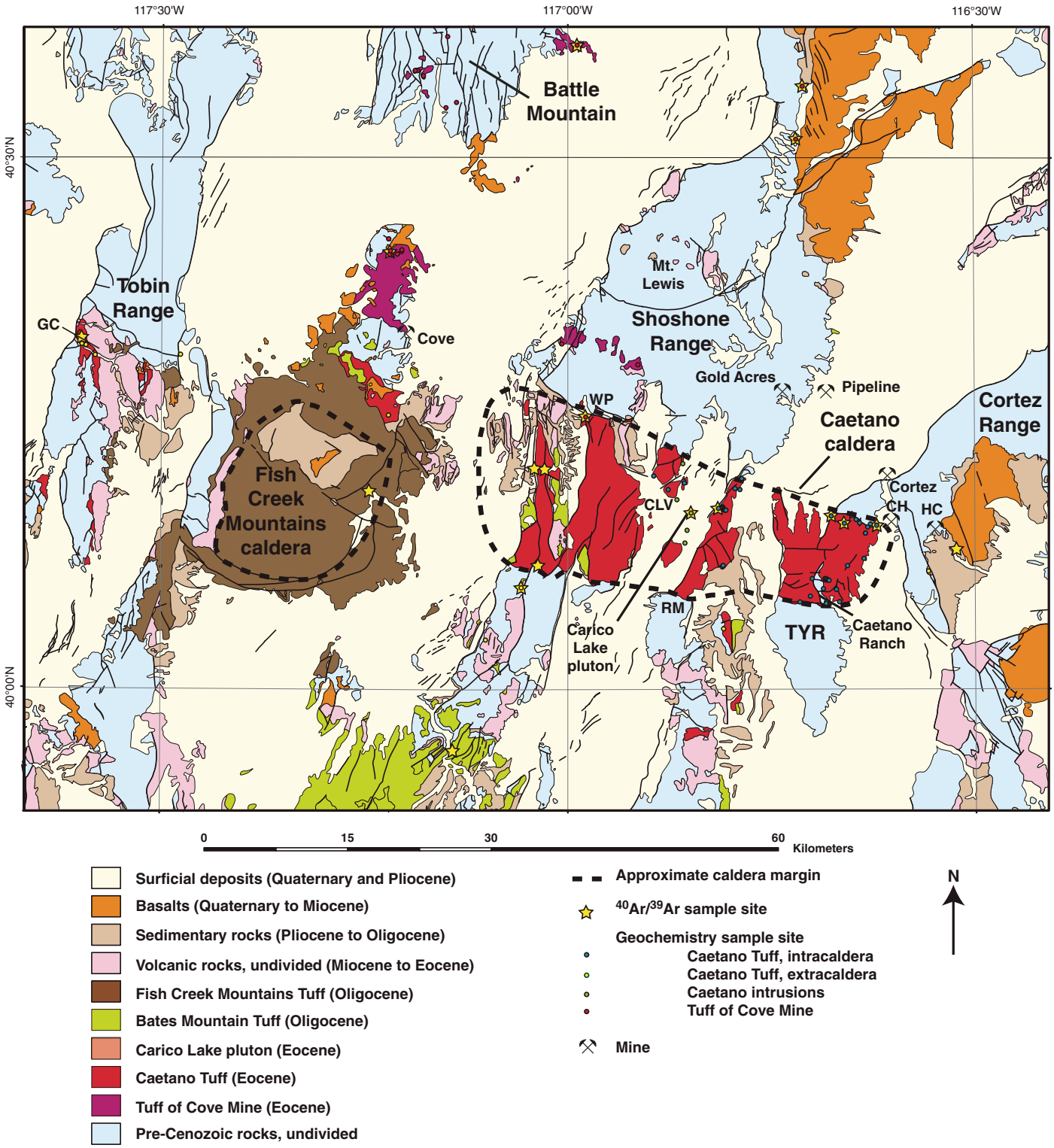

Figure 2. Generalized geologic map of the Caetano and Fish Creek Mountains calderas, showing distribution of the Caetano Tuff and tuff of Cove Mine and geochemical and geochronologic samples of this study. Geology modified from digital county geologic maps (Hess and Johnson, 1997) based on geologic maps for Lander, Churchill, Pershing, Humboldt, and Eureka Counties. CH—Cortez Hills deposit; CLV—Carico Lake Valley; GC—Golconda Canyon; HC—Horse Canyon mine; RM—Red Mountain; TYR—Toiyabe Range; WP—Wilson Pass.

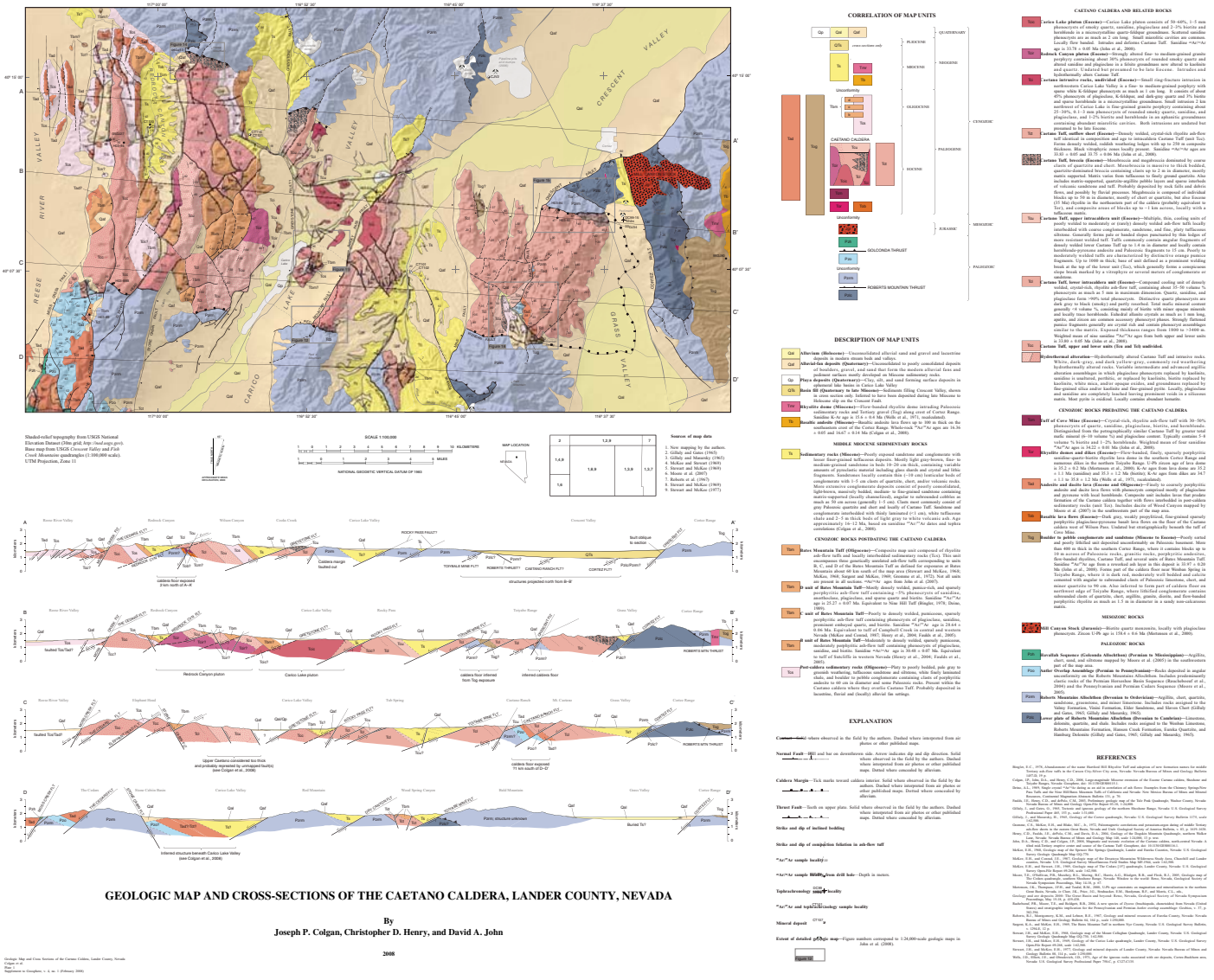

Plate 1. Colgan, J.P., Henry, C.D., and John, D.A., Geologic map and cross sections of the Caetano caldera, Lander County, Nevada, scale 1:100:000. If you are viewing the PDF of this paper or reading it offline, please visit http://dx.doi.org/10.1130/GES00115.S1 or the full-text article on www.gsajournals.org to view Plate 1.

carbonate rocks of the Antler overlap sequence (Roberts, 1964), which is exposed locally along the south margin of the caldera in the Shoshone Range (Plate 1; Moore et al., 2000) and underlies the caldera floor near Caetano Ranch in the Toiyabe Range (Fig. 4A). The Late Jurassic (ca. 158 Ma) granodioritic Mill Canyon stock intrudes the Paleozoic rocks in the Cortez Range just east of the caldera (Plate 1).

Cenozoic Pre-Caetano Tuff Rocks

Few Cenozoic rocks predating the Caetano Tuff are exposed in the vicinity of the Caetano caldera. Gravel deposits overlie Paleozoic basement on both the east and west ends of the caldera and locally form the caldera floor in the northern Toiyabe Range (Plate 1; Fig. 4B). These gravels are thought to fill a west-trending paleovalley now largely obscured by the Caetano caldera; evidence for this interpretation is discussed in a later section. Andesite or dacite lava flows are present locally between the gravels and the Caetano Tuff in the northern Toiyabe Range, and thin andesite or basalt flows underlie the caldera southwest of Wilson Pass in the Shoshone Range. Andesite flows interbedded with tuffaceous sedimentary rocks underlie outflow Caetano Tuff on the east side of the Fish Creek Mountains just west of the caldera (Fig. 2). Rhyolite dikes dated at 35.2 ± 0.2 Ma (U-Pb zircon, Mortensen et al., 2000) and a small rhyolite dome (K-Ar ages of 35.2 ± 1.1 Ma (sanidine) and 35.3 ± 1.2 Ma (biotite), Wells et al., 1971) intrude and overlie Paleozoic sedimentary rocks in the Cortez and Toiyabe Ranges just north of the caldera (Plate 1). Blocks of these rhyolites occur as breccia in the Caetano Tuff in the Toiyabe Range.

Caetano Tuff and Related Rocks

The Caetano Tuff is a phenocryst-rich, rhyolite ash-flow tuff widely exposed in north-central Nevada (Fig. 2; Gilluly and Masursky, 1965;

TABLE 1. SANIDINE SINGLE-CRYSTAL, $^{40}Ar/^{39}Ar$ AGES, CAETANO TUFF AND OTHER TUFFS, CAETANO CALDERA AREA

	Sample no.	Laboratory	Age (Ma)	±2σ	K/Ca	±2σ	n	MSWD	Latitude	Longitude	Reference
Caetano Tuff											
Intracaldera tuff											
Tilted Section, Cortez 15' Quadrangle, Toiyabe Range											
Highest exposed	00-DJ-34	New Mexico Tech	**33.79**	0.08	78.7	35.2	12	0.71	40.15633	–116.62136	This study
Highest exposed	00-DJ-34	New Mexico Tech	**33.81**	0.05	61.1	35.5	14	1.21	40.15633	–116.62136	This study
Middle	H03-82	New Mexico Tech	**33.82**	0.05	69.4	24.5	13	1.22	40.15868	–116.66343	This study
Lowest exposed	H03-84	New Mexico Tech	**33.71**	0.07	82.9	32.6	10	1.66	40.16440	–116.67692	This study
Other intracaldera											
Moss Creek Canyon, uppermost	H03-94	New Mexico Tech	**33.74**	0.05	69.5	21.1	14	0.39	40.20753	–117.02875	This study
Moss Creek Canyon, lowermost	05-DJ-14	New Mexico Tech	**33.84**	0.08	58.9	27.1	10	1.91	40.20856	–117.03818	This study
South of Rocky Pass, lowermost	05-DJ-27	New Mexico Tech	**33.85**	0.09	63.4	33.4	10	1.85	40.17145	–116.81544	This study
The Cedars Quadrangle, Shoshone Range	H03-88B	New Mexico Tech	**33.81**	0.08	82.5	29.9	9	1.63	40.11700	–117.03700	This study
Carico Lake Intrusion	H03-96	New Mexico Tech	**33.78**	0.05	55.7	16.2	15	1.02	40.16722	–116.84862	This study
Outflow tuff related to intracaldera tuff											
The Cedars Quadrangle, Shoshone Range	H03-89	New Mexico Tech	**33.83**	0.05	58.7	25.8	21	0.61	40.09663	–117.05763	This study
Golconda Canyon, Tobin Range	Tru5-4	New Mexico Tech	**33.75**	0.06			10	0.60	40.32450	–117.59367	Gonsior, 2006; this study
Reworked pyroclastic-fall tuff											
Horse Canyon, Cortez Range	99-DJ-80	USGS Menlo Park	**33.97**	0.20					40.13181	–116.52264	This study
Tuff of Cove Mine											
Base of section, Wilson Pass	06-DJ-13	New Mexico Tech	**34.21**	0.10	63.8	16.6	7	1.99	40.25761	–116.97843	This study
Elephant Head, south of Battle Mountain	H03-87	New Mexico Tech	**34.21**	0.07			9	1.30	40.60825	–116.98945	This study
Northern Fish Creek Mountains	05-DJ-8	New Mexico Tech	**34.22**	0.06	81.2	14.0	9	1.29	40.41410	–117.21910	This study
Mule Canyon Quadrangle, northern Shoshone Range	H00-53	New Mexico Tech	**34.23**	0.09	62.0	12.4	13	2.41	40.56940	–116.70849	This study
Mule Canyon Quadrangle, northern Shoshone Range	98-DJ-52	USGS Menlo Park	**34.45**	0.08					40.52222	–116.71694	John et al., 2000
Caetano-like tuff											
Outflow tuff, Bald Mountain	H03-108	New Mexico Tech	**35.10**	0.06	52	44.5	15	2.20	39.93107	–115.58870	This study
Reworked tuff, Alligator Ridge	–	USGS Denver	**35.22**	0.08					39.87333	–115.48333	Nutt, 2000
Non-Caetano tuffs											
Pyroclastic-fall tuff, Pipeline pit	CJV2	New Mexico Tech	**15.88**	0.10	1.6	1.0	8	0.29	40.24977	–116.72157	This study
Fish Ceek Mountains Tuff	H03-73	New Mexico Tech	**24.72**	0.05	21.0	6.8	15	0.56	40.18627	–117.24263	This study
Bates Mountain Tuffs at Reese River Narrows and New Pass											
D Nine Hill Tuff, New Pass	H00-78	New Mexico Tech	**25.27**	0.07	9.4	2.5	15		39.57637	–117.52721	This study
C Tuff of Campbell Creek	H01-139	New Mexico Tech	**28.64**	0.07	56	13.4	10		39.94438	–117.14159	This study
B Tuff of Sutcliffe	H01-138	New Mexico Tech	**30.48**	0.06	32	4.3	15		39.94491	–117.14183	This study
A Tuff of Rattlesnake Canyon	H01-137	New Mexico Tech	**31.03**	0.07	38	4.2	12		39.94438	–117.14296	This study

Note: Ages in bold are best estimates of eruption age. n = number of individual grains used to define weighted-mean age. Decay constants and isotopic abundances after Steiger and Jäger (1977). $\lambda_b = 4.963 \times 10^{-10}\ yr^{-1}$. $\lambda_e + e' = 0.581 \times 10^{-10} yr^{-1}$. $^{40}K/K = 1.167 \times 10^{-4}$. Minerals were separated from crushed, sieved samples by standard magnetic and density techniques; sanidine was leached with dilute HF to remove matrix and handpicked. Analyses at the New Mexico Geochronological Research Laboratory (methods in McIntosh et al., 2003). Samples were irradiated in Al discs for 7 hours in D-3 position, Nuclear Science Center, College Station, Texas. Neutron flux monitor Fish Canyon Tuff sanidine (FC-1). Assigned age = 28.02 Ma (Renne et al., 1998). Single sanidine grains were fused with a CO_2 laser operating at 10 W. Extracted gases were purified with SAES GP-50 getters. Argon was analyzed with a Mass Analyzer Products (MAP) model 215-50 mass spectrometer operated in static mode. Weighted-mean $^{40}Ar/^{39}Ar$ ages calculated by the method of Samson and Alexander (1987).

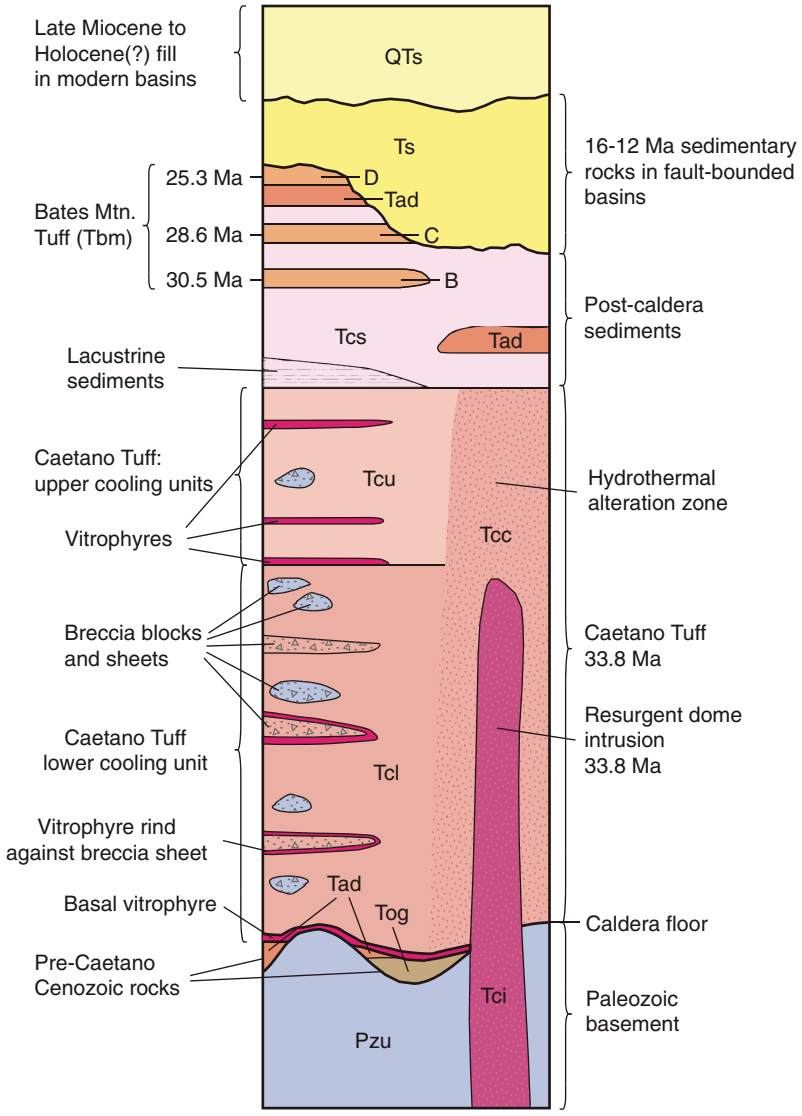

Figure 3. Generalized composite stratigraphic section for the Caetano caldera and post-caldera deposits filling the caldera. Unit symbols correspond to units in Plate 1. QTs—Quaternary and late Tertiary surficial deposits and basin fill; Ts—tuffaceous sedimentary rocks, sandstone, and conglomerate, undivided; Tbm—Bates Mountain Tuff; Tad—andesite and dacite lava flows; Tcs—Post-Caetano Tuff sedimentary rocks within the Caetano caldera; Tcb—megabreccia blocks and mesobreccia lenses in Caetano Tuff; Tcu—upper unit of the Caetano Tuff; Tcl—lower unit of the Caetano Tuff; Tcc—Caetano Tuff, undivided; Tci—granite porphyry intrusions related to Caetano Tuff; Tog—older gravel and conglomerate; Pzu—Paleozoic rocks, undivided.

Stewart and McKee, 1977; Burke and McKee, 1979; Gonsior, 2006). Petrographic, geochemical, and geochronologic data show that the Caetano Tuff as portrayed by Stewart and McKee (1977) consists of two distinct units: (1) an older outflow tuff on the north side of the caldera, erupted at ca. 34.2 Ma (probably from a northern source), and herein referred to as the tuff of Cove Mine, and (2) the main caldera-filling Caetano Tuff and related outflow tuff on the south and west sides of the caldera that erupted at ca. 33.8 Ma (Fig. 2). The two tuffs are in contact only near the north margin of the caldera southwest of Wilson Pass in the Shoshone Range, where 50–100 m of the tuff of Cove Mine overlies Tertiary basalt flows and is, in turn, overlain by intracaldera Caetano Tuff. Intrusive rocks related to the Caetano Tuff magmas intrude and locally deform and hydrothermally alter the central and western parts of the caldera (Plate 1).

Tuff of Cove Mine

The tuff of Cove Mine is named for prominent exposures at the north end of the Fish Creek Mountains, where a compound cooling unit of ash-flow tuff ~200 m thick fills a paleovalley that extends from the northern tip of the range to the Cove Mine (Figs. 2 and 4C; Stewart and McKee, 1977; Emmons and Eng, 1995). Other exposures of tuff that we correlate with the tuff of Cove Mine include outcrops in the south part of Battle Mountain (Roberts, 1964; Doebrich, 1995), Mill Canyon in the Shoshone Range (Gilluly and Gates, 1965), and the northwest corner of the Shoshone Range (John and Wrucke, 2003). The tuff of Cove Mine also forms part of the caldera floor and underlies intracaldera Caetano Tuff along the northwest edge of the caldera near Wilson Pass (Plate 1). The phenocryst-rich tuff of Cove Mine resembles the Caetano Tuff but is slightly older and more mafic with a greater abundance of mafic mineral phenocrysts (especially hornblende) and has a lower overall silica content.

Caetano Tuff

The Caetano Tuff is herein restricted to thick exposures of crystal-rich, rhyolite ash-flow tuff within the Caetano caldera (described below) and outflow tuffs south of the caldera in the Toiyabe and Shoshone Ranges, west of the caldera on the east side of the Fish Creek Mountains, and in Golconda Canyon in the Tobin Range (Fig. 2; Stewart and McKee, 1977; Gonsior, 2006). Gravels in the southwestern Cortez Range (unit Tog, Plate 1) also contain blocks of Caetano Tuff. The outflow tuffs are correlated with the Caetano Tuff on the basis of petrographic characteristics, geochemistry, and/or geochronology. We divide the intracaldera Caetano Tuff into two major units, separated by a complete cooling break and locally by thin sedimentary deposits. The lower unit is a single, compound, cooling unit as much as 3600 m thick in the northern Toiyabe Range. The upper unit consists of several, thin, cooling units interbedded with volcaniclastic sedimentary rocks and has a maximum exposed thickness of ~1000 m. The thickness of outflow Caetano Tuff varies widely, reflecting deposition over paleotopography, primarily into paleovalleys cut into the Eocene landscape. Outflow tuff is several hundred meters thick in the Toiyabe Range, ~30 km south of the caldera and in Golconda Canyon, ~40 km west of the caldera (Fig. 2).

Intracaldera Caetano Tuff is mostly densely welded and crystal rich, containing ~35–50 vol% phenocrysts as much as 5 mm in maximum dimension. Quartz, plagioclase, and sanidine generally form >90% of the total phenocrysts (Figs. 5 and 6). Quartz phenocrysts

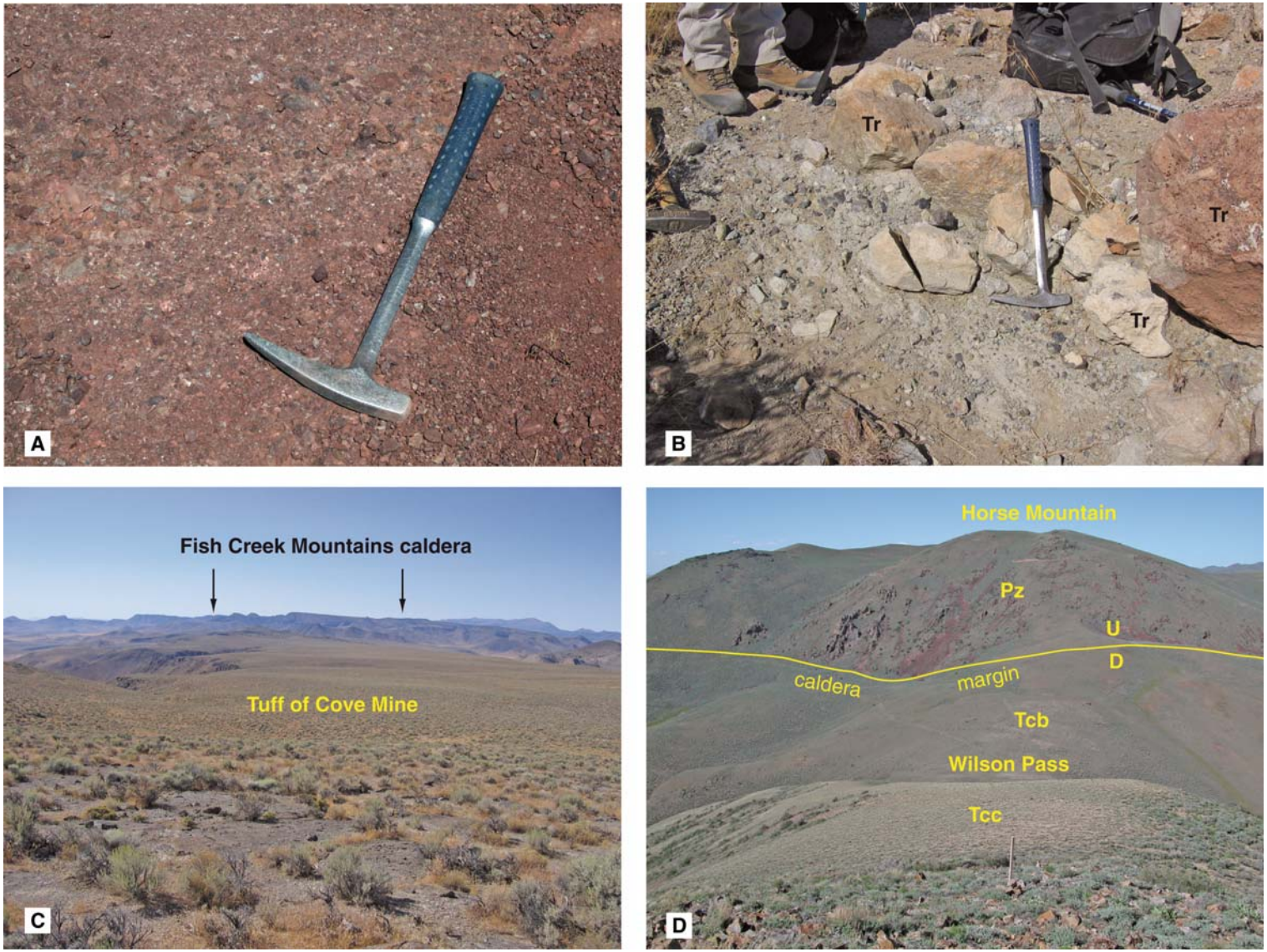

Figure 4. Photographs showing pre-Caetano caldera geology. (A) Chert-pebble conglomerate underlying caldera floor near Caetano Ranch in the northern Toiyabe Range. Rocks are thought to be part of the Pennsylvanian-Permian Antler Overlap sequence. Hammer is 46 cm long. (B) Middle Tertiary conglomerate forming caldera floor on northwest side of the Toiyabe Range. Well-lithified, non-calcareous conglomerate contains clasts of Paleozoic quartzite, chert, and argillite, Mesozoic(?) granite and diorite, and several textural types of Tertiary flow-banded rhyolite (Tr) up to 1.5 m in diameter. (C) View looking south along the crest of the north end of the Fish Creek Mountains. Questa in foreground is formed by flat-lying tuff of Cove Mine that fills a paleovalley. Higher part of range in background is comprised of Fish Creek Mountains Tuff that fills the younger Fish Creek Mountains caldera. (D) View north of Horse Mountain, Wilson Pass, and north margin of the Caetano caldera. Horse Mountain composed of Paleozoic quartzite and argillite (Pz). Caldera-bounding fault lies at base of talus slopes. Low area of Wilson Pass composed of poorly exposed mesobreccia (Tcb; Fig. 6D). Densely welded intracaldera Caetano Tuff (Tcc) forms ridge in foreground and dips ~40° east (right).

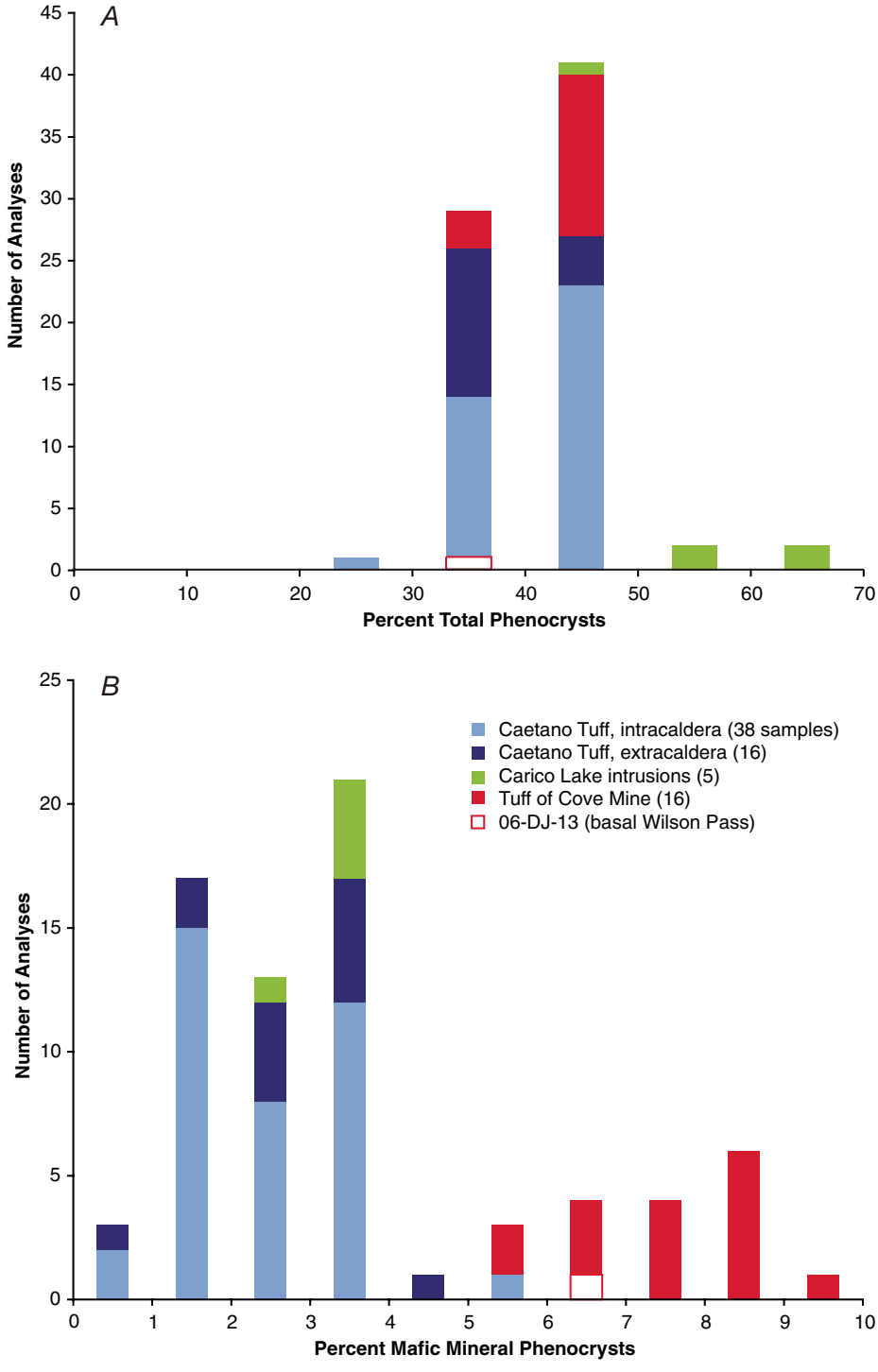

Figure 5. Histograms of modal data for the Caetano Tuff, tuff of Cove Mine, and Caetano caldera intrusive rocks. All analyses represent point counts of thin sections. Sample 06-DJ-13 is tuff that forms the caldera floor near Wilson Pass and is correlated with the tuff of Cove Mine. (A) Total phenocryst content. Lithic fragments were not counted. (B) Total mafic mineral phenocryst content.

commonly are dark gray to black (smoky) and partly resorbed. Total mafic mineral content generally is <4%. Biotite is the main mafic mineral, with trace amounts of hornblende present locally. Euhedral allanite crystals as much as 1 mm long, apatite, and zircon are common accessory phenocryst phases.

The lower unit of Caetano Tuff (map unit Tcl, Plate 1) is a compound cooling unit of relatively homogeneous, generally densely welded rhyolite and high-silica rhyolite ash-flow tuff (Fig. 7A). A 10–20-m-thick basal vitrophyre is preserved along the caldera floor in the northern Toiyabe Range (Fig. 7B), and numerous thin vitrophyric zones are irregularly distributed throughout the tuff in this part of the caldera (Gilluly and Masursky, 1965). Many of these vitrophyric zones envelop beds of mesobreccia or zones of tuff rich in lithic clasts (Fig. 7C), similar to vitrophyres quenched against mesobreccia in calderas in San Juan volcanic field (Hon and Lipman, 1989; Lipman, 2000, p. 27 and Fig. 7 therein). Nearly all other exposures of the intracaldera tuff are devitrified, and tuff in the western half of the caldera is hydrothermally altered. Clasts in the tuff include Paleozoic quartzite, chert, argillite, and limestone, granitic rocks, and Tertiary rhyolites, dacites, and andesites. Limestone, granite, and rhyolite clasts were only observed in the northern Toiyabe Range, near outcrops of the same rocks outside the caldera. Lithic content of the tuff varies significantly—Gilluly and Masursky (1965) described conglomerate beds in the tuff. These beds actually are zones of lithic-rich tuff (lag deposits) or non-tuffaceous mesobreccia that locally contain blocks of pre-caldera rocks as much as 5 m across (Fig. 7C). The pumice content of the tuff varies significantly, but nearly everywhere the crystal-rich pumice are strongly flattened (Fig. 7B) and generally <15 cm in maximum dimension.

The upper Caetano Tuff (map unit Tcu, Plate 1) lies above a pronounced welding break at the top of the lower unit (Fig. 8A) and locally is marked at its base by ~5 m of finely laminated, tuffaceous siltstone and sandstone. The upper unit consists of numerous, thin, ash flows interbedded with volcaniclastic siltstone, sandstone, and pebble conglomerate (Fig. 8B). Many of the ash flows are poorly welded and have undergone vapor-phase alteration, although thin, densely welded vitrophyres are present locally. The upper unit is widely exposed in the western half of the caldera (Plate 1), but both the upper and lower units are pervasively hydrothermally altered throughout these exposures and not everywhere distinguished on Plate 1. Exposures of relatively unaltered upper unit are best seen south of Rocky Pass along the crest and on the

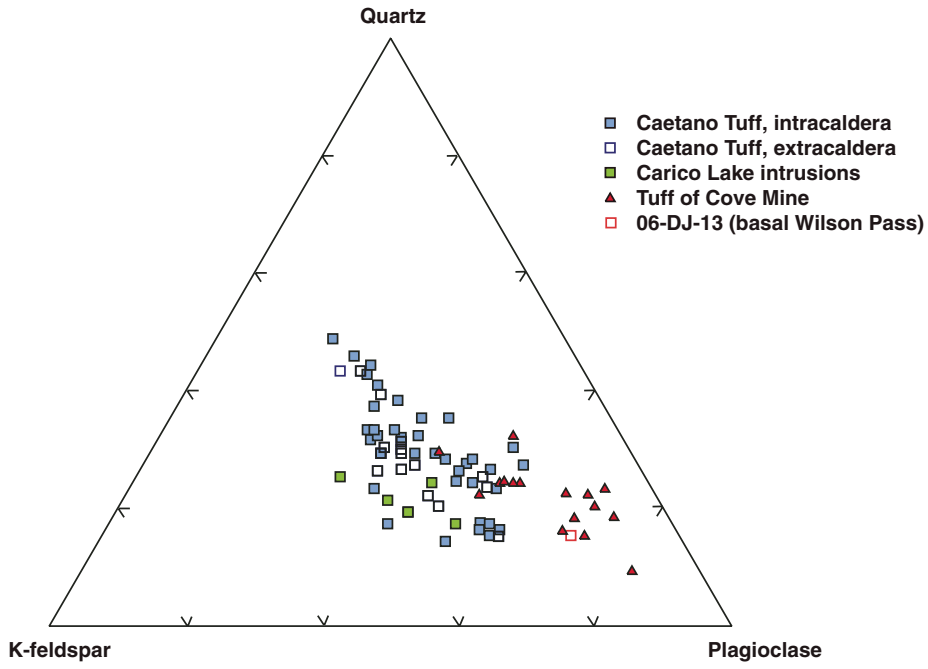

Figure 6. Ternary plot showing relative modal abundances of quartz, plagioclase, and K-feldspar phenocrysts in the Caetano Tuff, tuff of Cove Mine, and Caetano caldera intrusive rocks. All analyses represent point counts of thin sections.

east side of the ridge running south toward Red Mountain and in the low hills northwest of Tub Spring (Fig. 8C). In this area, the upper unit consists of multiple, thin, poorly to moderately welded ash flows locally containing abundant blocks of the densely welded lower unit (Fig. 8D). Thin (5–10 m) zones of more densely welded tuff within the poorly welded tuff indicate that the upper unit is composed of multiple, thin, cooling units that are petrographically and geochemically similar to the main (lower) unit.

Outflow tuffs correlated with the Caetano Tuff are found to the west and south sides of the caldera and as blocks in a gravel deposit (unit Tog, Plate 1) in the Cortez Range. They are generally moderately to densely welded and lithic poor, commonly with vitrophyric zones, notably in exposures south of the caldera. These tuffs are petrographically and geochemically similar to intracaldera Caetano Tuff (Figs. 5 and 6). In contrast, samples of the tuff of Cove Mine (previously mapped as Caetano Tuff) collected from the north side of the caldera in the northern Fish Creek Mountains, Battle Mountain, and northern Shoshone Range (Fig. 1) generally have significantly greater total mafic mineral (6–10%) and plagioclase contents than the intracaldera tuff. The tuff of Cove Mine typically contains 5–8 vol% biotite and 1–2% hornblende, compared to 1–3% biotite and 0–0.5% hornblende in the Caetano Tuff.

New $^{40}Ar/^{39}Ar$ dates, together with petrographic and geochemical data, demonstrate that the Caetano Tuff as previously mapped consists of two distinct tuffs that erupted at ca. 34.2 and 33.8 Ma. Nine samples of intracaldera and outflow Caetano Tuff were analyzed, including three samples from the northern Toiyabe Range that span nearly the entire stratigraphic thickness (>3.4 km) of intracaldera tuff, two samples from the lowest exposed intracaldera tuff at Moss Creek Canyon and south of Rocky Pass, and two samples of outflow tuff, one from 2 km southwest of the southwestern corner of the caldera and one from 45 km west of the caldera at Golconda Canyon (Fig. 2). They yielded ages ranging from 33.71 ± 0.07 to 33.85 ± 0.09 Ma (Table 1), with a mean and standard deviation of 33.79 ± 0.05 Ma. Ages from the two outflow samples fall within the range of the intracaldera samples (Table 1). A sample of pyroclastic-fall tuff in gravel in the Cortez Range dated at the U.S. Geological Survey (USGS) in Menlo Park is 33.97 ± 0.20 Ma. This age overlaps at 2σ with the Caetano Tuff ages determined at New Mexico Tech, and, thus, it may be related to the Caetano eruption, but this comparison and one for a sample of the tuff of Cove Mine from the northernmost Shoshone Range may be subject to a slight interlaboratory bias.

Ages of four samples from the tuff of Cove Mine, including one from the floor of the Caetano caldera near Wilson Pass (Fig. 2), range from 34.21 ± 0.10 (Wilson Pass) to 34.23 ± 0.09 Ma, with a mean and standard deviation of 34.22 ± 0.01 Ma. Figure 9 illustrates the distinct age difference between the Caetano Tuff and the tuff of Cove Mine, consistent with it being exposed below the Caetano Tuff. A sample of the tuff of Cove Mine dated at the USGS in Menlo Park is 34.45 ± 0.08 Ma. An additional sample from Caetano-like tuff collected at Bald Mountain 100 km east of the caldera (Fig. 1) yielded an age of 35.10 ± 0.06 Ma; thus, this sample is not related to either the Caetano Tuff or the tuff of Cove Mine.

Caetano Intrusive Rocks

Several bodies of granite porphyry intrude the central and west-central parts of the caldera (Plate 1). The largest intrusion is the ~25 km^2 Carico Lake pluton that intrudes the center of the caldera in Carico Lake Valley. The Carico Lake pluton consists of 55–65 vol%, 1–5 mm phenocrysts of smoky quartz, sanidine, plagioclase and 3–4% biotite and hornblende in a microcrystalline (0.05–0.1 mm) groundmass of quartz and feldspar. Sparse sanidine phenocrysts as much as 2 cm long are poikilitic and contain numerous plagioclase inclusions. Small miarolitic cavities are common. The pluton locally is strongly flow banded (Fig. 7D). The modal and chemical compositions of the pluton are similar to the Caetano Tuff, and it yielded a $^{40}Ar/^{39}Ar$ age of 33.78 ± 0.05 Ma, analytically indistinguishable from the Caetano Tuff that it intrudes (Table 1). The geochronologic data indicate that the maximum time between ash-flow eruption-caldera collapse and emplacement and cooling of the intrusion could therefore not have been more than ca. 0.1 Ma. The pluton appears to have domed the surrounding Caetano Tuff (as described below), and we interpret it as a resurgent intrusion of the magma that formed the Caetano Tuff.

The Redrock Canyon pluton intrudes the upper unit of the Caetano Tuff across the western part of the caldera between Redrock Canyon and Carico Lake Valley (Plate 1). It is exposed as scattered, strongly altered intrusive bodies that crop out in fault-bounded blocks, and it is inferred to be more extensive in the subsurface. The pluton is a medium-grained granite porphyry containing ~30%, 1–5 mm phenocrysts of rounded smoky quartz, tabular sanidine, and altered plagioclase and biotite in a felsite groundmass now altered to kaolinite and quartz.

A small, fine-grained, holocrystalline granite porphyry intrudes the north margin of the caldera at the north end of Carico Lake Valley and is interpreted as a ring-fracture intrusion. It consists of ~45 vol% phenocrysts composed of

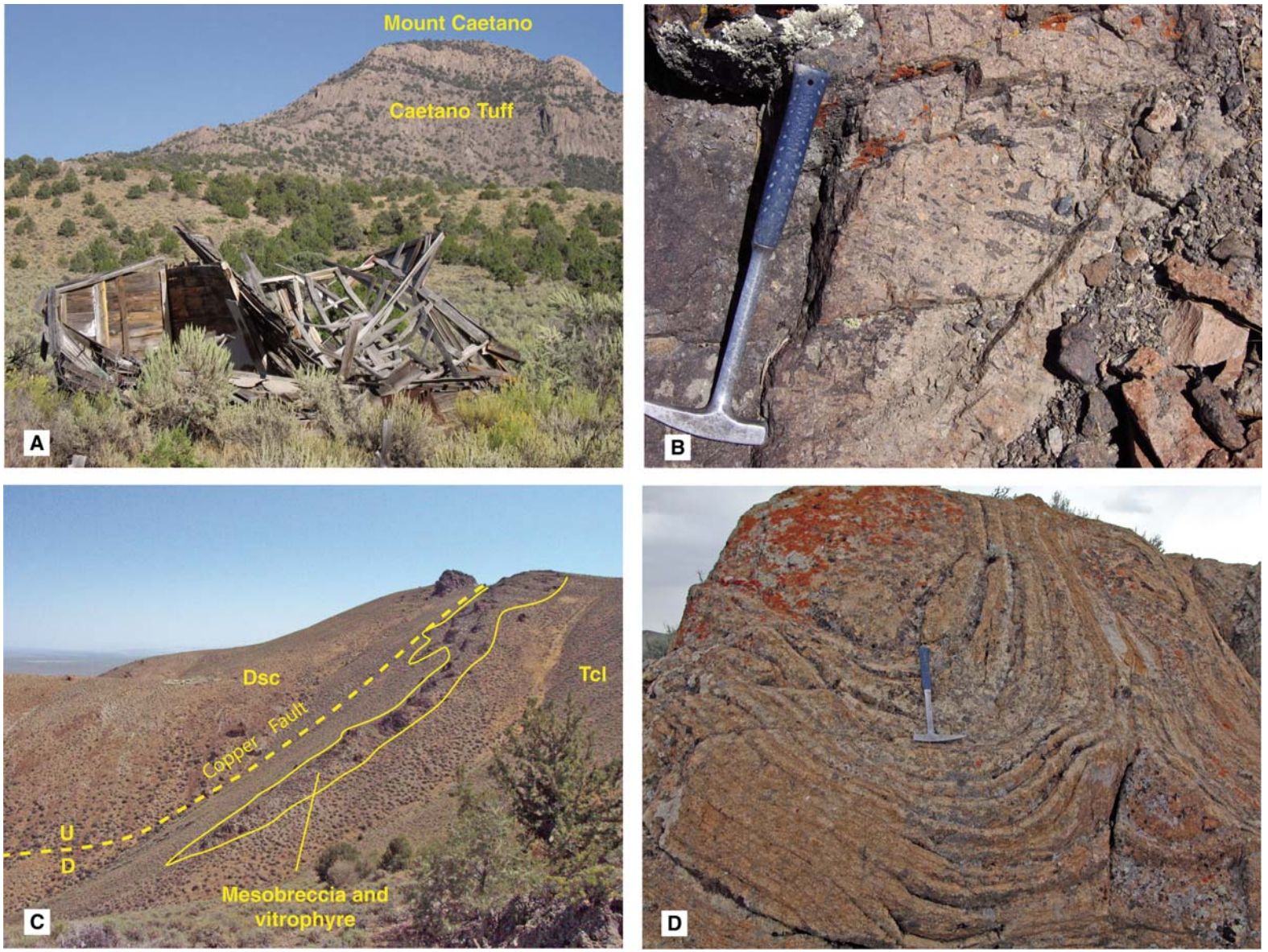

Figure 7. Photographs showing aspects of the Caetano caldera and Caetano Tuff. (A) View of Mount Caetano looking east. Mount Caetano is composed of densely welded lower unit of the Caetano Tuff that dips ~40–45° east (away) from photo. Total topographic relief is ~500 m. Remains of Caetano Ranch in foreground. (B) Strongly flattened crystal-rich pumice (fiamme) in densely welded basal vitrophyre in Caetano Tuff near Wenban Spring in northern Toiyabe Range. Hammer is 46 cm long. (C) View looking north of caldera margin in northern Toiyabe Range. Devonian Slaven Chert (Dsc) faulted against intracaldera Caetano Tuff (Tct) along the Copper Fault. Lens of mesobreccia in Caetano Tuff is enveloped by black vitrophyre thought to have formed by quenching of hot ash against cold breccia blocks shed into the caldera during eruption. (D) Flow bands in Carico Lake pluton. Hammer is 46 cm long.

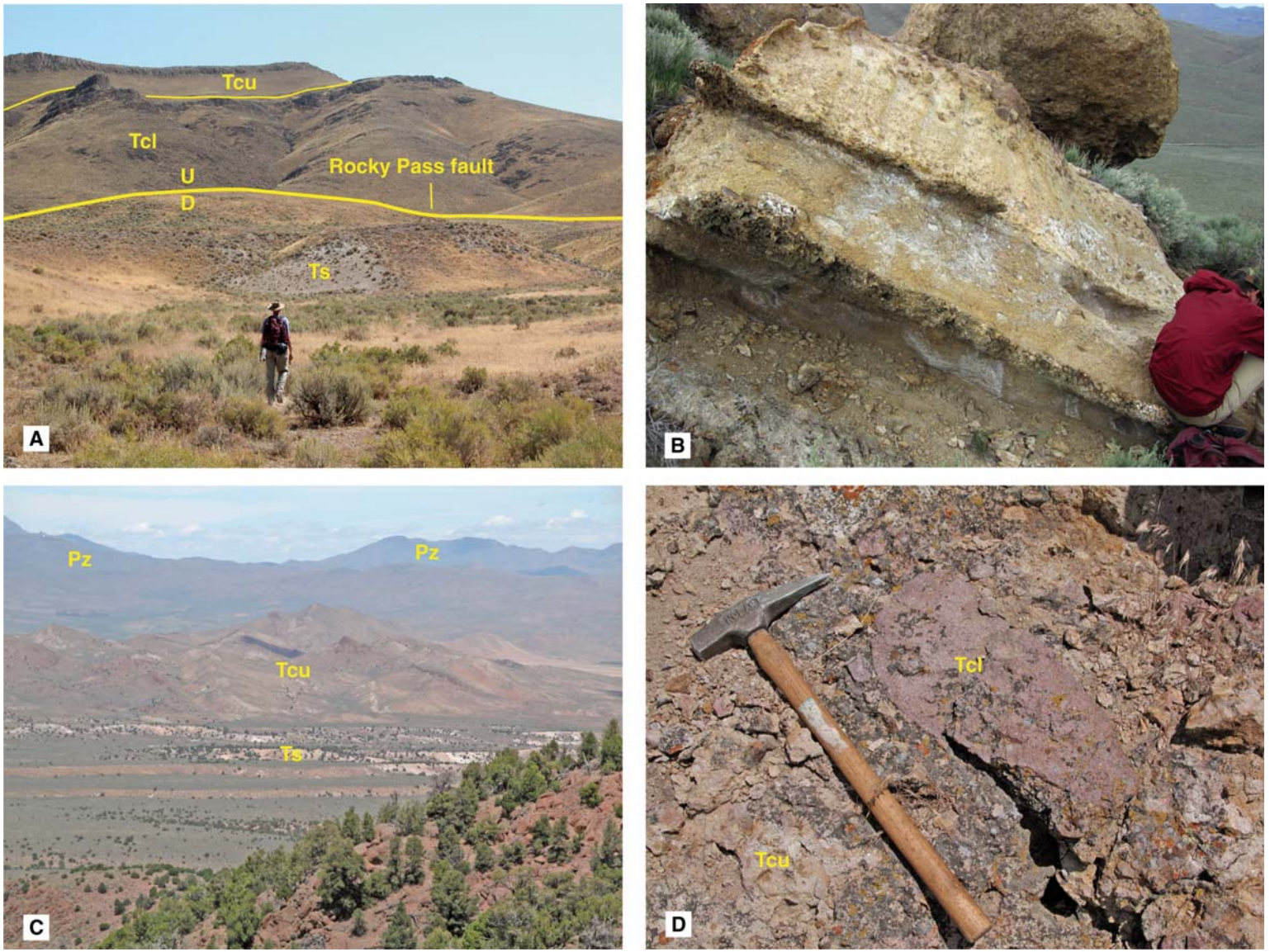

Figure 8. Photographs showing aspects of the upper unit of the Caetano Tuff. (A) View east of prominent cooling break between lower (Tcl) and upper (Tcu) units of Caetano Tuff along west side of ridgeline ~2 km south of Rocky Pass. Low hills in foreground composed of middle Miocene sedimentary rocks (Ts) deposited in hanging wall of the Miocene Rocky Pass fault. Ridgeline is ~300 m above valley floor. (B) Hydrothermally altered volcaniclastic sandstone and pebble conglomerate beds in upper unit of Caetano Tuff on south side of Wilson Canyon near Redrock Canyon. White recessively weathered beds are kaolinite altered, whereas dark resistant beds are silicified. (C) View north of multiple fault blocks of the upper unit of the Caetano Tuff (Tcu) in the low hills southeast of Rocky Pass and Paleozoic rocks (Pz) forming skyline in the Shoshone Range. White rocks on valley floor are syn-extensional, middle Miocene sedimentary rocks (Ts) that unconformably overlie the caldera (Colgan et al., 2008). Dips of these sedimentary rocks shallow upward to the east (Plate 1). Densely welded outflow Caetano Tuff crops out in the foreground. (D) Block of densely welded lower Caetano Tuff (Tcl) in lithic-rich poorly welded lower part of upper Caetano Tuff (Tcu) northwest of Tub Spring. Hammer handle is ~55 cm long.

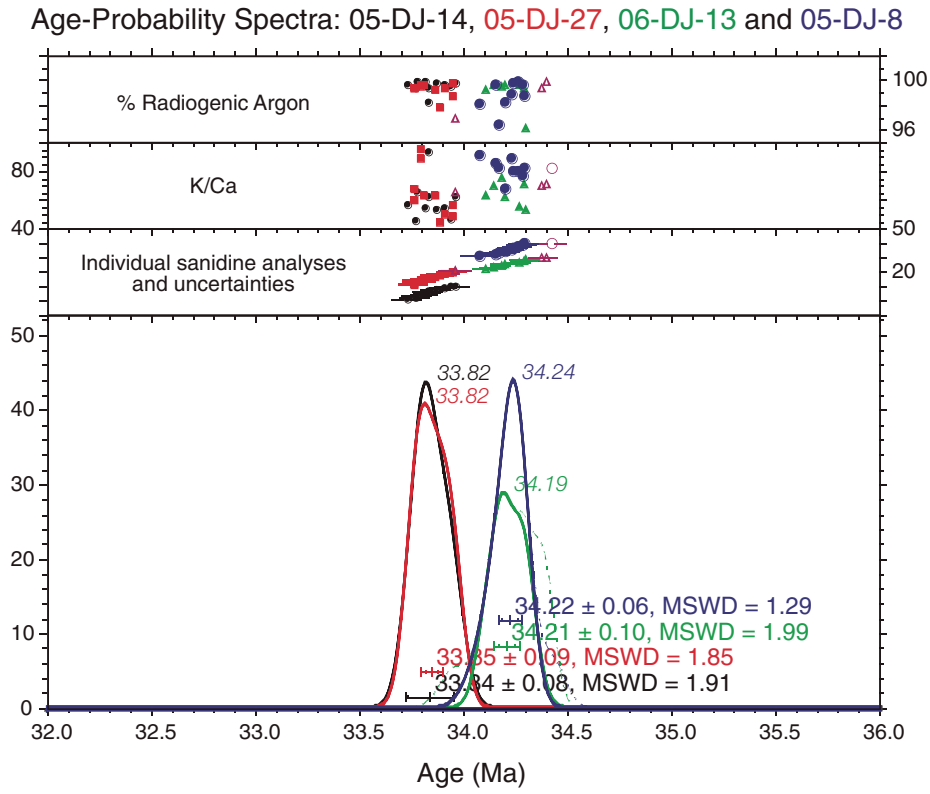

Figure 9. $^{40}Ar/^{39}Ar$ single-crystal data in age probability diagrams of two samples each of Caetano Tuff (05-DJ-14, 05-DJ-27) and tuff of Cove Mine (06-DJ-13, 05-DJ-8) showing distinctly different ages of each. Unfilled data points were not used in age calculation.

subhedral to euhedral plagioclase, K-feldspar, and dark-gray, rounded to strongly resorbed quartz in a microcrystalline felsic groundmass. The intrusion contains sparse, white K-feldspar phenocrysts as much as 1 cm long. Mafic phenocrysts comprised of biotite, opaque minerals, and trace amounts of hornblende form ~3% of the intrusion. Sparse, small (<1 mm) miarolitic cavities are present.

Geochemistry of the Caetano Tuff, Related Intrusive Rocks, and the Tuff of Cove Mine

The Caetano Tuff and the tuff of Cove Mine are subalkaline rhyolites using total alkali-silica relations and the IUGS (International Union of the Geological Sciences) chemical classification (Fig. 10; Irvine and Baragar, 1971; Le Bas et al., 1989). Normalized silica contents range from 68.7 to 77.5 wt% SiO_2. Five samples of the Carico Lake pluton and the ring-fracture intrusion have 71.3–73.3 wt% SiO_2. Total alkali ($Na_2O + K_2O$) contents of all samples are mostly between 7.5 and 8.5 wt%.

The tuffs clearly separate into two compositional groups with different trends of major and trace elements: (1) high-silica intracaldera and extracaldera Caetano Tuff from west, south, and east sides of the caldera, and (2) more mafic, lower silica tuff of Cove Mine from the north side of the caldera (Fig. 10). The tuff of Cove Mine has notably higher Mg, total Fe, Ti, and P contents and lower Al, Ba, and Zr contents relative to the Caetano Tuff at the same silica content. These chemical data corroborate the separation of the extracaldera tuffs into two groups defined by their petrographic and modal characteristics and $^{40}Ar/^{39}Ar$ ages, and suggest that extracaldera tuffs from the west, south, and east sides of the caldera are related to intracaldera Caetano Tuff.

Chemical analyses of intrusive rocks in Carico Lake Valley are generally similar to the intracaldera Caetano Tuff (Fig. 10). Silica contents of the intrusive rocks are similar to the mafic parts of the intracaldera tuff, and major and trace element contents generally lie on the same compositional trends as the intracaldera tuffs, consistent with them being genetically related. The Redrock Canyon pluton is pervasively altered, and we have no chemical analyses of it.

Chemically analyzed samples of intracaldera Caetano Tuff can be projected onto cross sections to estimate their relative stratigraphic position within the caldera and allow examination of general compositional trends within intracaldera tuff (Fig. 11). The intracaldera tuff reaches a maximum observed thickness of ~3400 m in the northern Toiyabe Range (just south of the Copper Fault, Plate 1), but neither the upper unit nor the caldera floor are exposed in this section. We assume that the caldera floor is very close to the exposed base of this section, consistent with exposures a few km to the south in the footwall of the Caetano Ranch Fault (Plate 1). We next assume that the cooling break between the upper and lower units is just above the top of the exposed section, buried beneath younger sediments in Grass Valley; this yields a thickness of ~3600 m for the lower unit. No single fault block exposes both the caldera floor and the top of the upper unit; therefore, we estimate the stratigraphic position of our samples relative to either the cooling break between the upper and lower units or the exposed caldera floor. They are plotted on Figure 11 relative to their inferred stratigraphic height (in meters) above the caldera floor. Varying the assumed thickness of the lower cooling unit will thus stretch the vertical axis of the Figure 11, but will not change the relative position of the plotted samples.

The basal (vitrophyric) Caetano Tuff exposed along the caldera floor in the northern Toiyabe Range is high-silica rhyolite containing 76.2–76.4 wt% SiO_2. The lower ~2800 m of the intracaldera tuff shows little compositional zoning with high silica contents (76.0–77.7 wt% SiO_2) throughout. Samples collected near the top of the lower unit in the northern Toiyabe Range, Tub Spring, Rocky Pass, and Carico Lake Valley areas all have markedly lower silica contents, 71.8–73.5 wt% SiO_2, than samples from the lower part of the tuff. Silica contents of the upper unit range from 71.9 to 75.6 wt%, overlapping silica contents of the upper part of the lower unit and extending to higher values. Silica content increases abruptly ~1.5–2 wt% from the lower to upper units in the Rocky Pass section.

Combined stratigraphic and geochemical data for intracaldera Caetano Tuff and related intrusive rocks suggest four major trends. (1) Thick, relatively homogeneous, high-silica rhyolite (76–78 wt% SiO_2) forms most of the intracaldera tuff. (2) More mafic rhyolite compositions (72–74% SiO_2) comprise the upper ~700 m of the lower unit, indicating overall normal compositional zoning upward in this single compound cooling unit. (3) The upper unit tends to be more silicic than the upper part of the lower unit, but overall it displays a wider range of compositions, probably reflecting smaller volume, less widespread (?) eruptions. (4) The Carico Lake pluton and the ring-fracture intrusion have compositions (71–73% SiO_2) overlapping to slightly more mafic than the upper part of the lower unit,

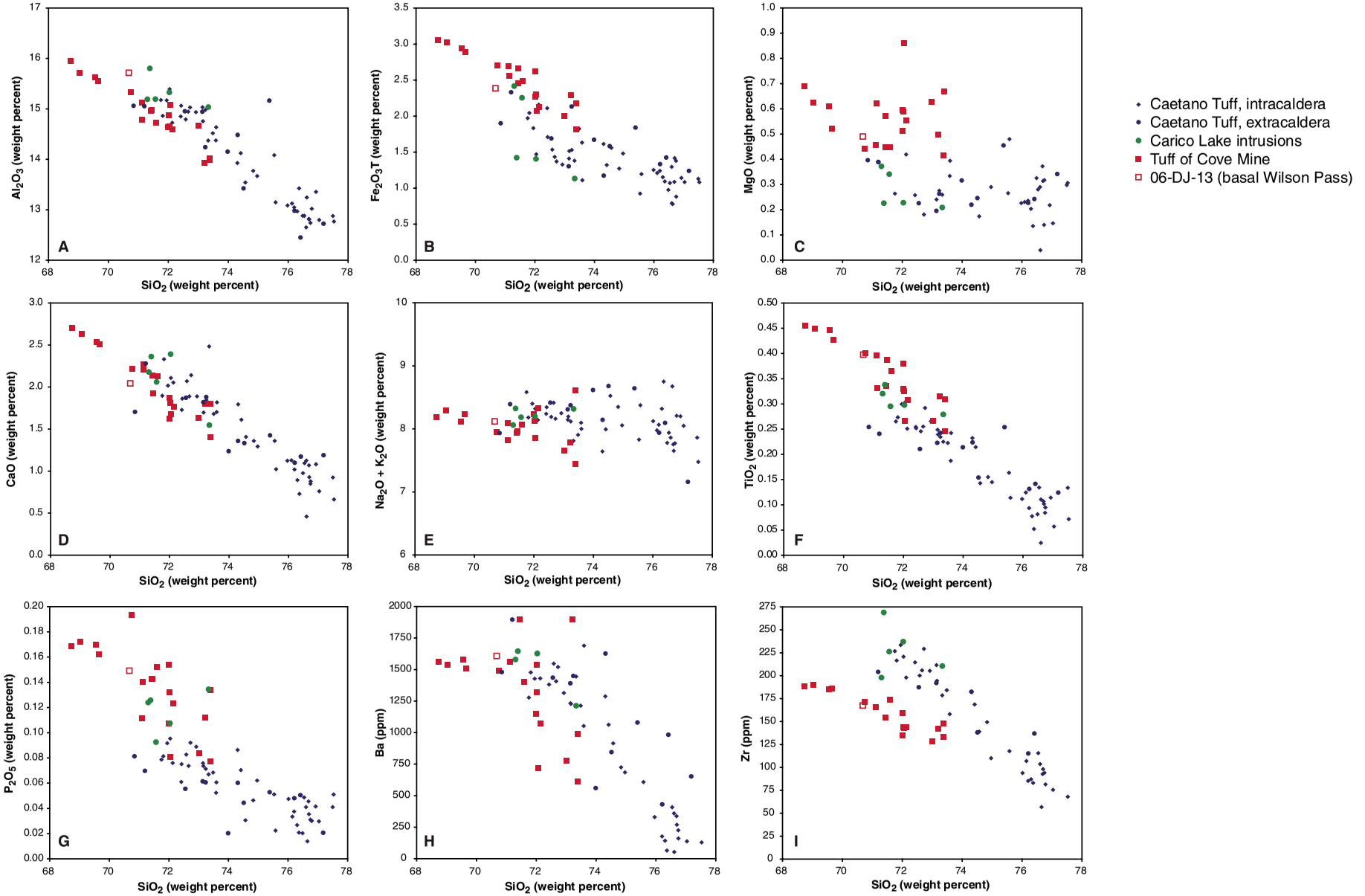

Figure 10. Silica variation diagrams for whole-rock samples of the Caetano Tuff, tuff of Cove Mine, and Caetano caldera intrusive rocks. Major elements normalized to 100% volatile free. See text for data sources. (A) Al_2O_3-SiO_2; (B) Fe_2O_3T-SiO_2; (C) MgO-SiO_2; (D) CaO-SiO_2; (E) Na_2O+K_2O-SiO_2; (F) TiO_2-SiO_2; (G) P_2O_5-SiO_2; (H) Ba-SiO_2; (I) Zr-SiO_2.

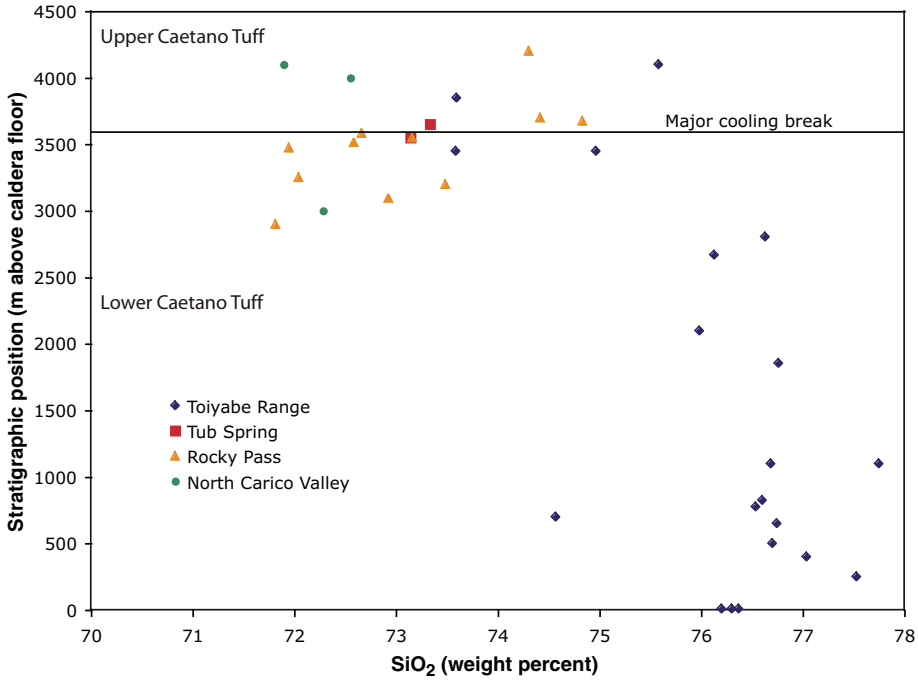

Figure 11. Plot of silica content versus stratigraphic position (height above caldera floor) for intracaldera Caetano Tuff. See text for description of how stratigraphic position was calculated and assumptions inherent in these estimates.

suggesting that these intrusions represent residual, deeper (?) parts of the magma that erupted forming the lower Caetano Tuff.

Post-Caldera Sedimentary Rocks and Ash-Flow Tuff

The depression resulting from caldera collapse served as a long-lived depocenter for sedimentary rocks and distal outflow tuffs (unit Tcs, Plate 1). The sedimentary rocks crop out extensively in the western part of the caldera and locally in the Toiyabe Range. A lower part of these sedimentary rocks consists of platy tuffaceous sandstone, siltstone, and white shale, probably deposited in a shallow lake shortly after caldera collapse and resurgence. The upper part of this unit consists of several repeated sequences of pebble conglomerate that grade upward over a few tens of meters to fine sandstone.

Interbedded with the sedimentary rocks are several ash-flow tuffs collectively referred to as the Bates Mountain Tuff, named for exposures at Bates Mountain ~60 km south of the caldera (Stewart and McKee, 1968; McKee, 1968). Much has been published about the Bates Mountain Tuff in central Nevada (e.g., Sargent and McKee, 1969; Best et al., 1989), and the most recent stratigraphic subdivision recognizes four ash-flow cooling units, A through D (Grommé et al., 1972). Detailed mapping and other studies, mostly in western Nevada, show that these tuffs have distinct ages and are unrelated, and the four tuffs have been assigned individual formal and informal names (Table 1; Bingler, 1978; Best et al., 1989; Deino, 1989; Henry et al., 2004; Faulds et al., 2005). Units B (tuff of Sutcliffe), C (tuff of Campbell Creek), and D (Nine Hill Tuff) form 5–20-m-thick ledges in the caldera, although not every tuff is present in every section. Unit A (tuff of Rattlesnake Canyon) has been found only as clasts in gravel in the Cortez Range but may be present in sections not examined in detail for this study. Sanidine $^{40}Ar/^{39}Ar$ ages reported in Table 1 from Reese River Narrows and New Pass, 35 and 80 km, respectively, southwest of the Caetano caldera, range from 31.03 ± 0.07 Ma (unit A, tuff of Rattlesnake Canyon) to 25.27 ± 0.07 Ma (unit D, Nine Hill Tuff) and are representative of ages determined for the tuffs regionally (Deino, 1989; Henry et al., 2004; Faulds et al., 2005).

All four units of the Bates Mountain Tuff have been found in the Sierra Nevada in California, ~300 km west of the Caetano caldera (Brooks et al., 2003; Henry et al., 2004). Unit D is particularly widespread, occurring from near Ely, Nevada, to the western foothills of the Sierra Nevada, a distance of 500 km (Deino, 1989). Unit C erupted from a caldera in the Desatoya Mountains (McKee and Conrad, 1987; Henry et al., 2004), ~120 km to the southwest. Sources for the other units are unknown.

Miocene Sedimentary Rocks

Middle Miocene sedimentary rocks are exposed irregularly through the caldera (Figs. 8A and 8C). These rocks consist of fine-grained, tuffaceous sandstone and shale with abundant tephra layers, and coarser alluvial-fan deposits of sandstone and conglomerate (Colgan et al., 2008). They are interpreted to have been deposited in localized hanging-wall basins during the Miocene extensional faulting that broke up the Caetano caldera. Colgan et al. (2008) report new $^{40}Ar/^{39}Ar$ ages and tephrochronologic data for tephras interbedded in these rocks, indicating deposition of the sediments mostly between ca. 16 and 12 Ma.

CALDERA ORIGIN OF THE CAETANO TUFF

Our reinterpretation of the Caetano trough as an ash-flow caldera has important consequences for the regional tectonic and magmatic history of the study area (Table 2). In the following section, we review field relationships from key localities where the Caetano caldera displays thick intracaldera tuff, steep caldera margins where pre-caldera and intracaldera units are abruptly truncated against each other, megabreccia and mesobreccia, a resurgent dome/intrusion, and a ring-fracture intrusion (Plate 1). These features are characteristic of well-documented, ash-flow calderas worldwide and indicate rapid eruption of ash-flow tuff from an underlying shallow magma chamber, coeval collapse of the chamber roof-caldera floor, ponding of the tuff within the caldera, and slumping of the caldera walls during and shortly following caldera collapse (Smith and Bailey, 1968; Lipman, 1984, 1997).

Red Mountain Caldera Margin

The caldera margin, thick intracaldera ash-flow tuff, and coarse mesobreccia are well exposed north of Red Mountain along the south-central margin (Fig. 12). The caldera margin, which strikes west-northwest and dips steeply northward, separates Ordovician Valmy Formation on the south from interbedded intracaldera tuff and mesobreccia on the north. Both the Valmy Formation and Caetano Tuff strike generally north to northeast, dip moderately eastward, and are truncated abruptly at the margin. Measured dips in Caetano Tuff vary from 23 to 44°, and the section is repeated by a northwest-dipping fault, so the exposed thickness is unknown but is probably ~500–600 m. The tuff

TABLE 2. CHARACTERISTICS OF ASH-FLOW CALDERAS AND VOLCANO-TECTONIC TROUGHS

	Calderas	Volcano-tectonic troughs
Primary map shape	Generally approximately equant	Highly elongate
Cross section	Symmetrical subsidence	Half graben rather than graben?
Evidence for regional extension perpendicular to trough (long axis)	Not necessary	Essential
Boundary	Near vertical faults around entire caldera	Extensional faults might dip ~65°; faults bound sides, not ends
Ash-flow tuff character	Thick, relatively homogeneous, possibly vertically zoned	Thick, possibly heterogeneous, if trough formed over long time
Megabreccia and mesobreccia	Common	Common?
Resurgent intrusion	Common	Unknown?
Interbedded tuff, lava, and sedimentary rocks	No interbedded lava. Sedimentary rocks include only mesobreccia and megabreccia or sedimentary deposits interbedded with tuff deposited during the waning stages of the caldera cycle.	Potentially common, if trough formed over long time
Other volcanic fill	Caldera collapse phase should have only ash-flow tuff and breccia; post-collapse could have abundant late lavas and sedimentary rocks.	Lavas and sedimentary rocks could be throughout section
Rapid subsidence coeval with ash flow eruption	Characteristic origin	Yes, but could be several episodes separated by long times
Examples	Many hundreds worldwide	Panther Creek, Challis field, Idaho

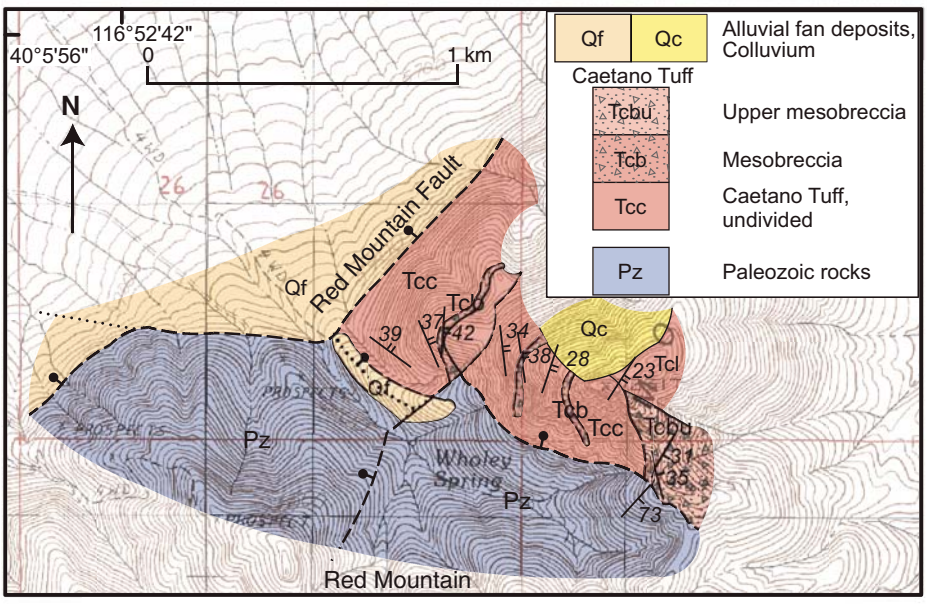

Figure 12. Geologic map of the southern caldera margin at Red Mountain (Wood Spring Canyon 7-½' quadrangle). East-dipping Caetano Tuff and interbedded mesobreccia lenses composed of Paleozoic clasts (Fig. 13A) are abruptly truncated against Paleozoic Valmy Formation at west-northwest–striking, steeply north-dipping caldera margin. Upper mesobreccia consists of interbedded lenses of Paleozoic clast debris-flow deposits and lithic-rich Caetano Tuff (Fig. 13B). The Red Mountain fault steps abruptly westward at and probably reactivates the caldera boundary fault.

is mostly densely welded and strongly altered, with feldspar and biotite phenocrysts altered to kaolinite. Lithic fragments are generally sparse, but are locally abundant immediately above several mesobreccia lenses and in poorly welded tuff near the top of the ridge.

Several lenses of mesobreccia are interbedded with tuff. They are 5–10 m thick and are composed of angular, clast- to matrix-supported clasts up to 50 cm in diameter (Fig. 13A). Most lenses are massive and unsorted, but one lens has irregular zones characterized by different clast sizes. The zones are nonplanar and commonly strongly oblique to layering in the surrounding ash-flow tuff. Clasts in the lower breccia lenses are almost entirely Paleozoic quartzite and argillite, with sparse Tertiary andesite. Upper lenses also contain clasts of Caetano Tuff and pumice up to 50 cm in diameter. Matrix in all lenses consists of finely ground Paleozoic rocks. Lithic-rich tuff overlies one of the uppermost mesobreccia lenses with sharp contact.

The capping mesobreccia (unit Tcb, Fig. 12) consists of a heterogeneous mix of massive to moderately well-bedded, very coarse to fine deposits. The massive deposits are mostly similar to the interbedded lenses but contain angular quartzite clasts up to 1 m in diameter. Lag blocks of quartzite up to 2 m in diameter were probably eroded out of breccia deposits.

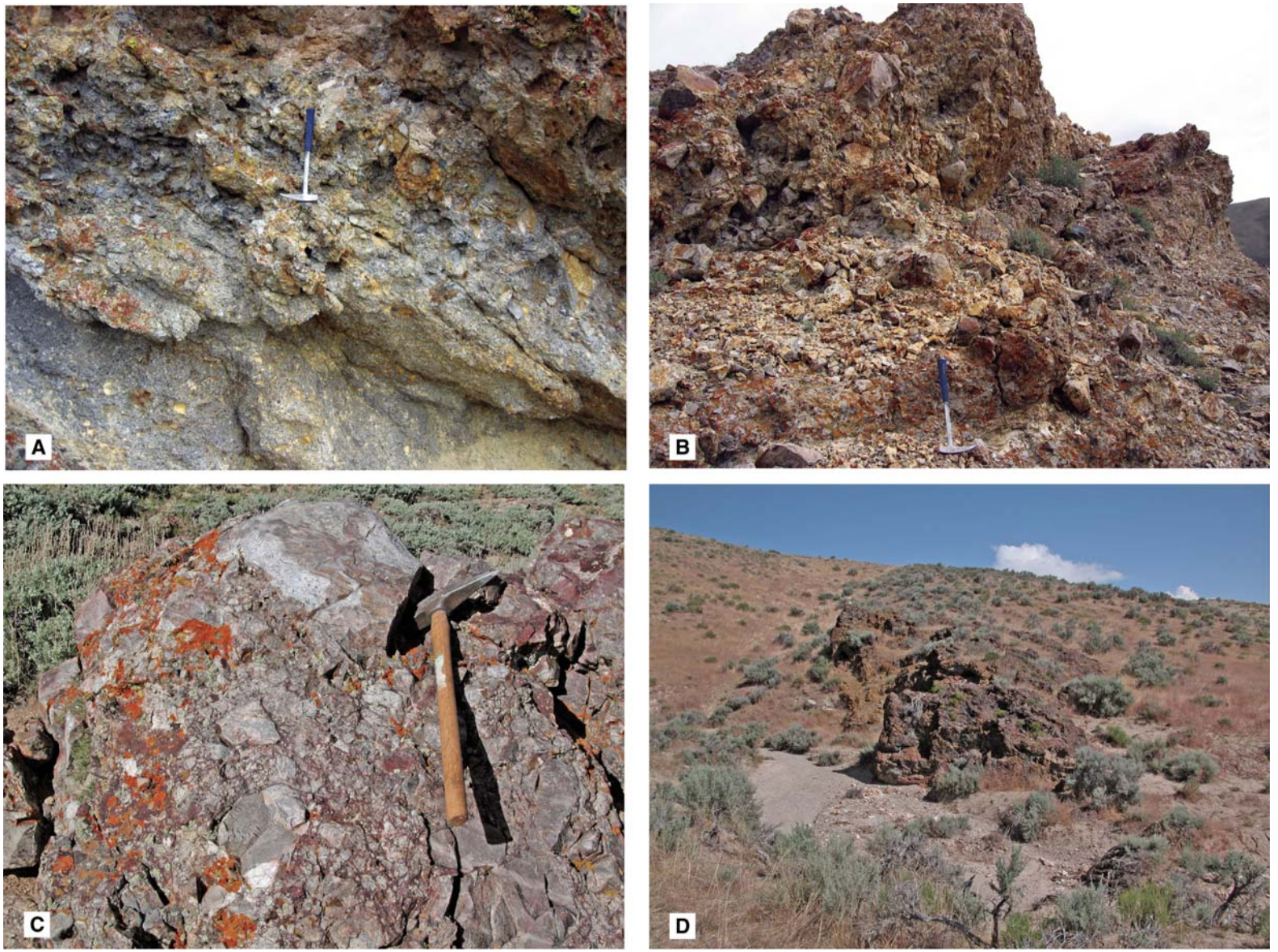

Figure 13. Photographs showing breccias in the Caetano caldera. (A) Approximately 10-m-thick mesobreccia lens in lower unit of Caetano Tuff near south margin of caldera just north of Red Mountain. Mesobreccia composed of angular fragments (up to 50 cm) of Paleozoic quartzite, argillite, and chert, Tertiary andesite, and white pumice in matrix of finely ground Paleozoic rocks. Hammer is 46 cm long. (B) Interbedded coarse, clast-supported mesobreccia and lithic-rich Caetano Tuff near south margin of caldera north of Red Mountain. Blocks are mostly Paleozoic quartzite and argillite and locally reach 2 m in diameter. Hammer is 46 cm long. (C) Brecciated Paleozoic quartzite block in mesobreccia at Wilson Pass. Hammer is 55 cm long. (D) Large block of brecciated Paleozoic chert enclosed in Caetano Tuff near base of upper unit ~0.5 km north of Tub Spring. Block is ~5 m in maximum dimension and is ~4 km from the nearest exposed caldera margin.

Sequences of coarse breccias consist of several layers, which, individually, are one to 5 m thick. A few layers show faint internal bedding, and a few layers have tuff matrix, demonstrating that they are very lithic ash-flow tuffs. Finer deposits consist of moderately to well-bedded, pebbly to coarse, volcanic sandstone, with pebbles of quartzite (Fig. 13B).

We interpret the high-angle contact between Paleozoic rocks and tuff and mesobreccia to be the caldera margin. The margin originated as a fault scarp resulting from caldera collapse and, given its steepness, is probably close to the actual fault plane. However, the contact is not exposed, and debris was shed from the margin during caldera collapse, thus much of the margin is eroded topographic wall. The structurally lower, western parts of the margin probably are closer to the actual fault than are structurally higher, eastern parts. The mesobreccia lenses within the tuff probably are rock falls or avalanches from the caldera wall, and the capping mesobreccia probably is a mix of rock fall and avalanche deposits, as well as primary ash-flow tuff, debris-flow deposits, and minor fluvially reworked tuff and breccia. The paucity of coarse lithics in most intracaldera tuff indicates that there was little erosion of the vent during tuff eruption and that most mesobreccia was deposited by abrupt rock falls that interacted little with the enclosing tuff that was being deposited. In contrast, the complex stratigraphy of the upper mesobreccia and the presence of a few layers with tuff matrixes suggest that the upper mesobreccia was deposited near the end of tuff eruption.

The caldera margin has been reactivated by, or influenced the location of, the Red Mountain fault that bounds the east side of modern Carico Lake Valley (Fig. 12). This fault, which has prominent scarps suggesting late Quaternary offset, strikes north-south but turns abruptly westward, where it intersects the caldera margin, probably following the margin. The fault turns back to a more northeasterly strike ~700 m to the west.

Wilson Pass Caldera Margin

The north margin of the caldera is exposed at Wilson Pass (Fig. 14) and displays several features different from those at Red Mountain. Thick, intracaldera tuff and megabreccia are present, but the margin itself is more structurally

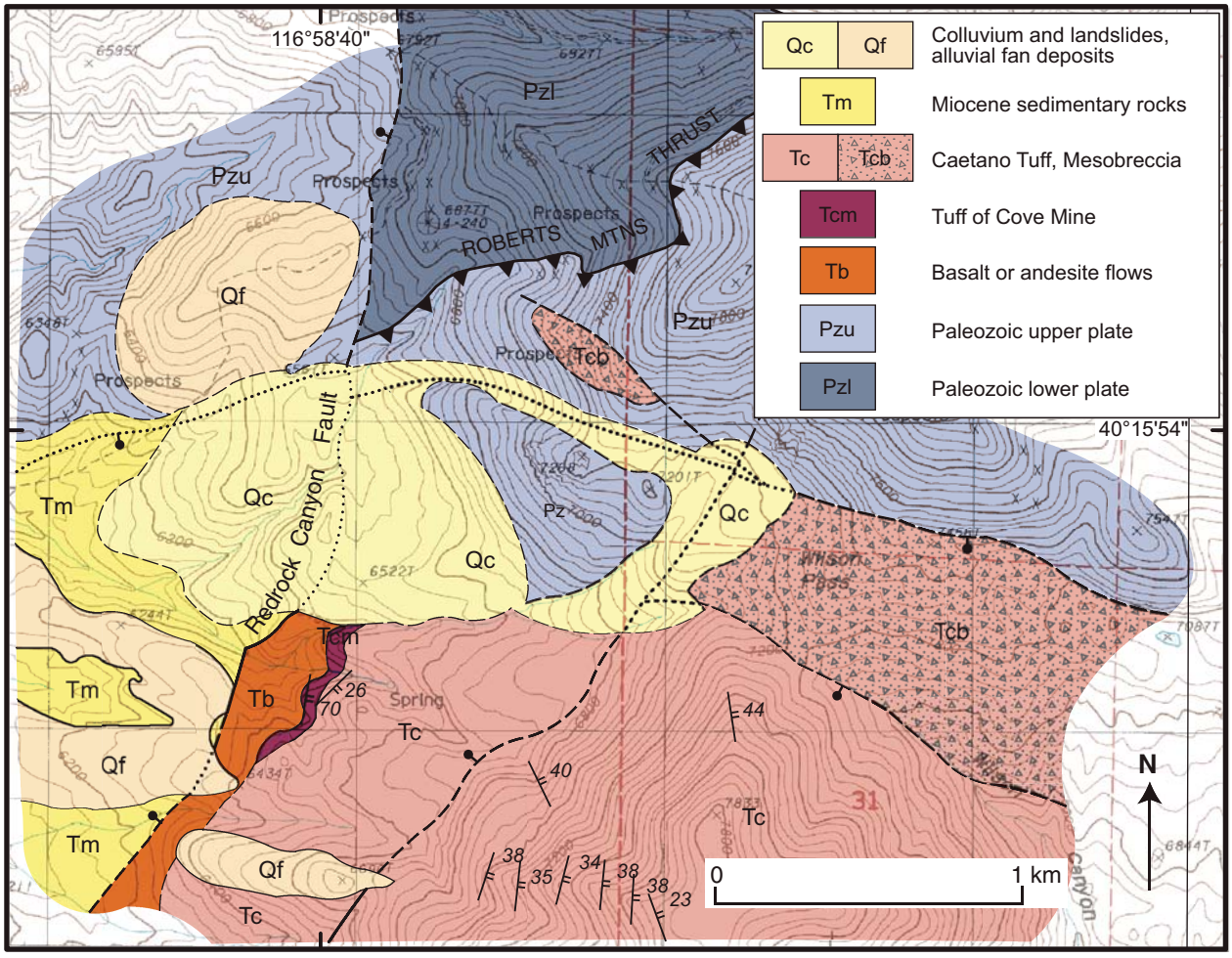

Figure 14. Geologic map of the northern caldera margin at Wilson Pass (Goat Peak 7-½' quadrangle). Caldera boundary probably consists of two west-northwest–striking, steeply dipping faults separating Paleozoic rocks north of the northern fault, mesobreccia between the two faults, and Caetano Tuff south of the southern fault (Figs. 4D and 7D). Paleozoic rocks at Peak 7268 may be megabreccia or part of caldera wall. Caetano Tuff overlies the caldera floor consisting of tuff of Cove Mine underlain by basalt lava flows. Miocene sedimentary rocks (Tm) were deposited in the hanging wall of the middle Miocene Redrock Canyon fault (Colgan et al., 2008).

or erosionally complicated. The caldera margin strikes west-northwest and dips steeply south. Gilluly and Gates (1965) mapped two fault strands. Paleozoic rocks exposed in or near the margin, north of the north strand, include upper plate chert, quartzite, and lesser sandstone and shale. Mesobreccia and probable megabreccia are poorly to well exposed between the two strands (Figs. 4D and 13C). Intracaldera tuff crops out south of the south strand, dips 30–45° east, and directly overlies an exposure of the caldera floor consisting of mafic lava flows and the older tuff of Cove Mine (Fig. 14). The intracaldera tuff here is ~1800 m thick. Despite its proximity to the caldera margin, the Caetano Tuff in this area contains only sparse, small lithics and no breccia lenses. The tuff is altered but less so than at Red Mountain; plagioclase is generally altered to kaolinite, and biotite is locally altered to white mica or kaolinite, but sanidine generally is unaltered.

Mesobreccia at Wilson Pass consists of blocks of variably brecciated quartzite and argillite in soil that locally contains pieces of Caetano Tuff (Fig. 4D). Breccia matrix is not exposed in this area; therefore, it is uncertain whether the tuff pieces are clasts or weathered from matrix. The largest clasts are themselves brecciated, with angular, monolithologic, clast-supported pieces of quartzite or argillite to 35 cm in an indurated, probably siliceous matrix. Well-exposed mesobreccia that consists of matrix-supported, angular to subrounded pieces of argillite, quartzite, sandstone, and chert in a finely granular matrix appears to rest depositionally on Valmy quartzite northwest of Wilson Pass. A large, coherent outcrop of chert west of Wilson Pass (Fig. 14) may be a large breccia block or an intact part of the caldera wall.

The Wilson Pass caldera margin could consist of two fault strands, as mapped by Gilluly and Gates (1965), or the northern strand could be eroded caldera wall and the southern strand closer to an actual structural margin. If the latter, mesobreccia between the two strands would be resting on intact caldera wall, similar to the well-exposed mesobreccia (Tcb 1 km northwest of Wilson Pass, Fig. 14). However, the steepness and linearity of the northern strand suggests it is a fault. The absence of lower plate Paleozoic rocks in breccia indicates that lower plate rocks were not exposed in the topographic caldera wall at the time of caldera collapse.

Northeastern Caldera Margin—The Copper Fault

The northeastern part of the caldera in the Toiyabe Range shows thick intracaldera tuff, an exposed caldera boundary fault, an upward transition from boundary fault to topographic wall resulting from major slumping of the wall, and megabreccia and mesobreccia (Fig. 15, Plate 1). The average dip of the Caetano Tuff is 40° indicating that exposed intracaldera tuff here is ~3400 m thick. The base of the tuff is not exposed but is probably not far below the lowest exposed tuff given exposure of the caldera floor ~7 km to the south (see section Caldera Floor at Caetano Ranch); therefore, we assign a thickness of 3600 m for the lower unit of the Caetano Tuff. Because the tuff and caldera are tilted, a transect east along the caldera margin is an oblique upward transect along the original margin.

The western half of the northeastern caldera margin mapped by us coincides with the Copper Fault of Gilluly and Masursky (1965). This western part is probably the caldera structural boundary where intracaldera tuff is faulted against Paleozoic rocks. For example, at A (Fig. 15), a planar, 58°, southward-dipping fault surface is developed in resistant Devonian Slaven Chert, which makes a low ridge on the north against less resistant tuff and breccia on the south (Fig. 16A). Chert is intensely brecciated along the fault. Caetano Tuff crops out ~30 m to the south but is not exposed along the fault surface.

Megabreccia and mesobreccia are interbedded with Caetano Tuff from the Copper Fault, the northern margin, southward to near the Wenban Fault, the southern margin (Figs. 15 and 16A). Breccia near A consists of a single chert megabreccia ~30 m long with brecciated margins and several lenses of mesobreccia containing clasts of Paleozoic chert, quartzite, and chert-pebble conglomerate up to ~2 m in diameter (Figs. 7C, 16A, and 16B). Caetano Tuff forms vitrophyre adjacent to many of the mesobreccia lenses (Fig. 7C).

The caldera structural boundary is especially well exposed at B, ~1 km east of A (Fig. 15). At this location, densely welded, highly sheared Caetano Tuff is in a sharp, vertical to steeply south-dipping contact with chert in the margin (Fig. 16B). Pumice is highly stretched, parallel to the contact, to the point the rock resembles flow-banded rhyolite (Fig. 16C). Adjacent chert is brecciated and tightly recemented. Faulting probably occurred while the tuff was still hot and could deform ductily, but adjacent chert was brittle either because it was colder or compositionally distinct (all SiO_2). The attitude of Caetano Tuff away from the margin changes progressively to the normal north-northeast strike and moderate east-southeast dip, but even 50 m from the caldera margin tuff dips to the south as steeply as 87° (Fig. 15). These relationships suggest the tuff was both deposited against the chert and also downfaulted along it. Tuff deposited against chert partly stuck to it but also underwent internal shearing during caldera subsidence; tuff farther from the chert was simply dragged down to its steep southward dip with little or no shearing. The exposed contact, its topographic expression, and the steep dips in tuff show that this structural boundary dips vertically to steeply southward (Figs. 16B and 16C).

Mesobreccia lenses at the stratigraphic level of B in the central part of the caldera contain clasts of limestone and finely, sparsely porphyritic, flow-banded feldspar-quartz-biotite rhyolite, in addition to quartzite, chert, and chert-pebble conglomerate. Individual blocks are as large as 5 m. Several limestone and quartzite blocks have brecciated and recemented margins (Fig. 17A). Where exposed, matrix consists of finer clasts, but many lenses occur as trains of blocks with no exposed matrix.

East of B (Fig. 15), the caldera margin continues nearly due east, whereas the Copper Fault of Gilluly and Masursky (1965) turns slightly to the south to follow what we interpret as the boundary between massive, relatively lithic-poor Caetano Tuff to the south and megabreccia-rich tuff to the north. The caldera margin as mapped by us separates intact Devonian Slaven Chert on the north from megabreccia, which consists of numerous large blocks and clusters of blocks, mostly of chert, in a poorly exposed matrix of Caetano Tuff. Because chert is so much more resistant than tuff, it dominates outcrop and makes up all the hills and knobs (Fig. 16D), thus Gilluly and Masursky's (1965) interpretation that it is Paleozoic rock in place. The four large areas of upper plate Paleozoic rocks south of the caldera margin shown in Figure 15 are composite, consisting of numerous individual blocks up to at least 50 m in diameter. A few natural outcrops and several mining-related exposures show irregular "fingers" and thicker lenses of tuff through the composite blocks. Lithic-rich tuff crops out in low areas between blocks (Fig. 16D), but much of the area of unit Tcx consists of breccia blocks of all sizes in a clayey soil with grains of quartz, sanidine, and biotite from disaggregated tuff. The northern caldera margin is not exposed but can be located within a few meters in several locations where tuff gives way to coherent Paleozoic rock. This part of the northeastern caldera margin is probably the eroded topographic wall, where megabreccia slumped from the wall during ash-flow eruption and caldera collapse.

Megabreccia consists mostly of chert, but sparsely porphyritic, flow-banded rhyolite also is common. Gilluly and Masursky (1965) mapped several rhyolite bodies as in-place intrusions

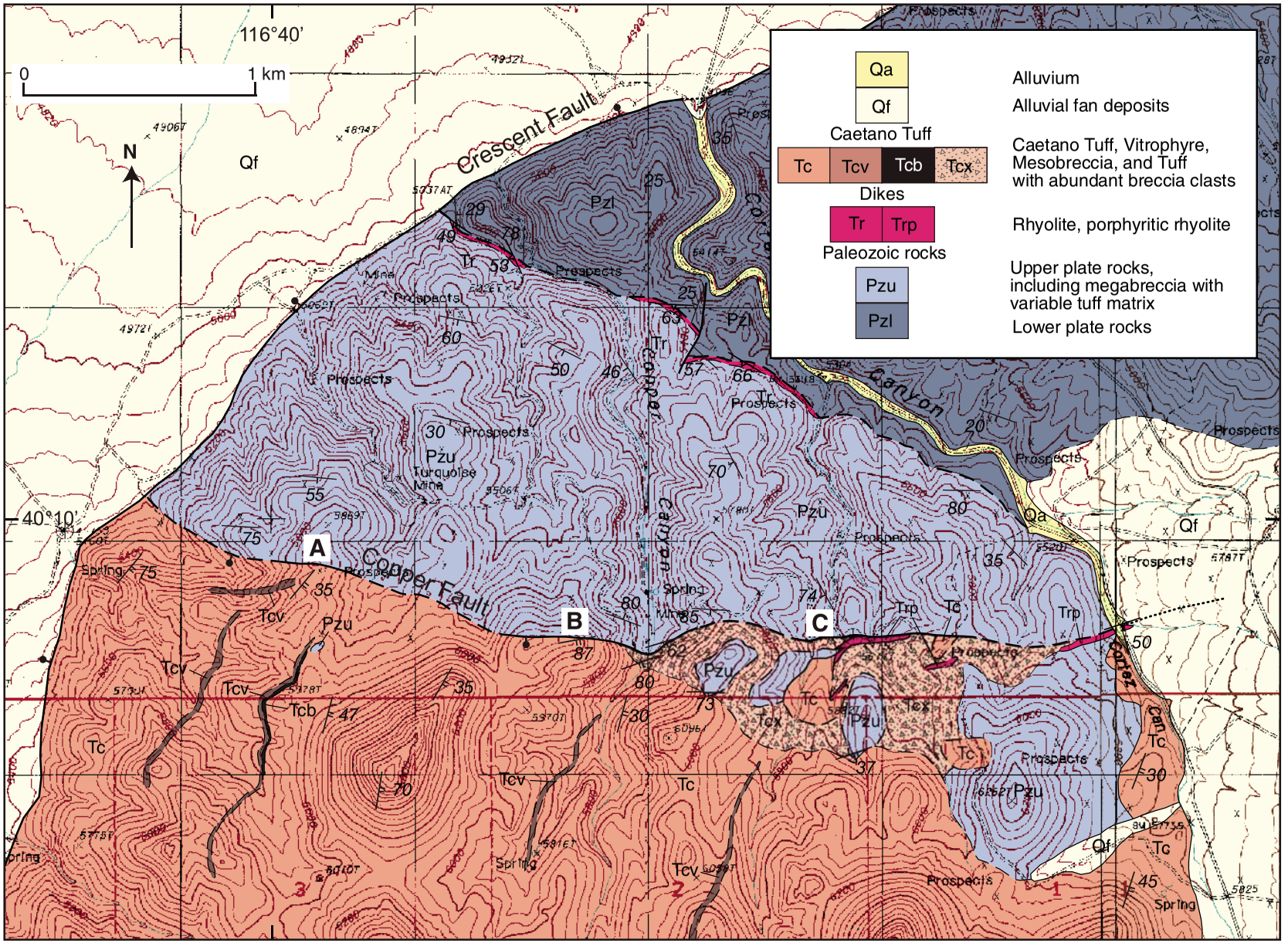

Figure 15. Geologic map of the northeastern caldera margin (Cortez and Cortez Canyon 7-½' quadrangles). East-dipping intracaldera Caetano Tuff is at least 3400 m thick in this area. Intracaldera breccia varies from scattered lenses of mesobreccia containing clasts up to ~2 m in diameter in the western, stratigraphically and structurally lowest part of the caldera to abundant megabreccia composed of individual blocks up to 50 m in diameter and composite areas of blocks up to ~1 km across in the eastern, highest part of the caldera. The caldera margin in the western part of the figure is a fault that constitutes the structural margin. The eastern part of the caldera margin is eroded, topographic wall from which the exposed megabreccia slumped into the caldera. Locations A, B, and C are discussed in the text.

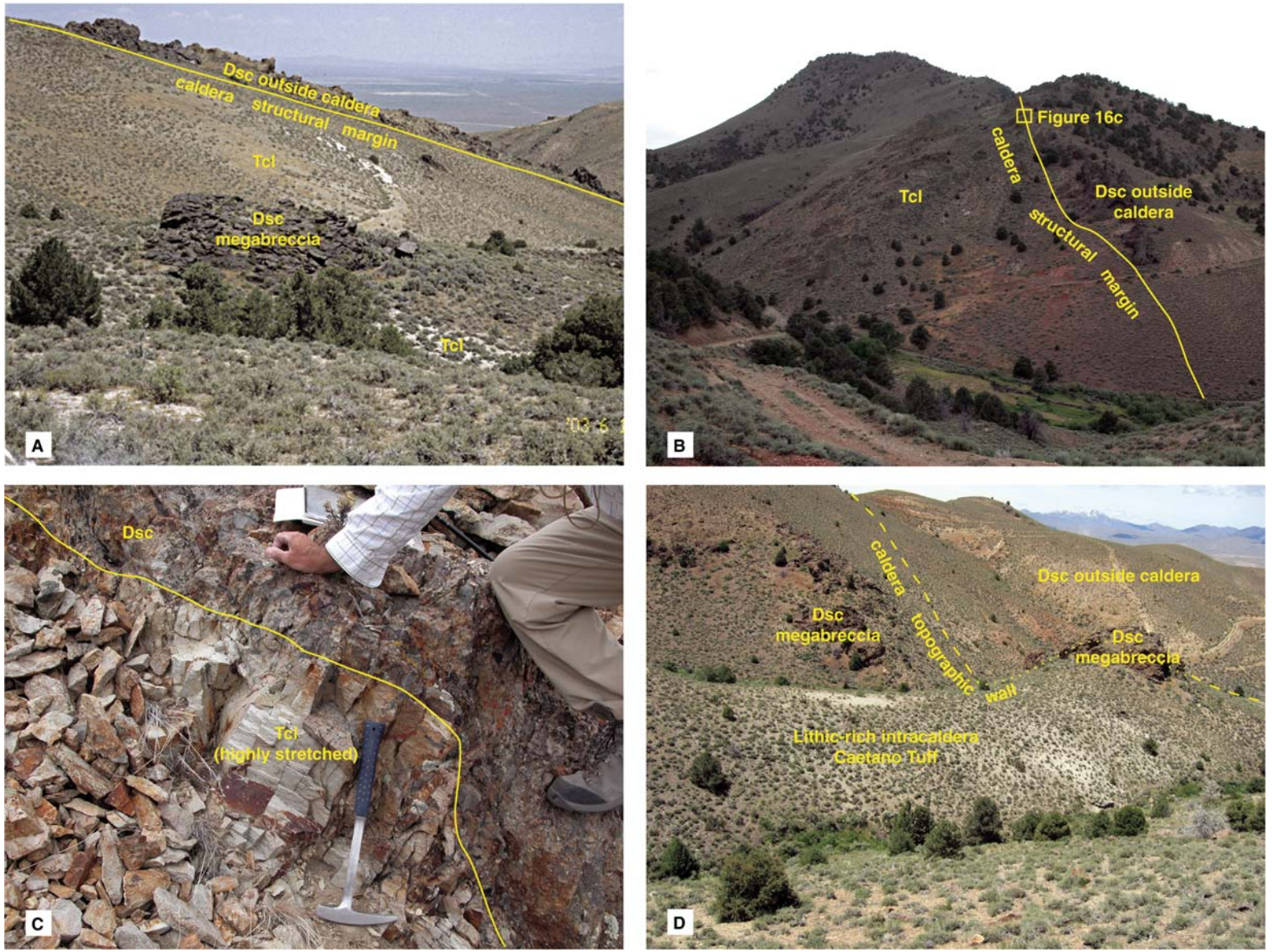

Figure 16. Photographs showing the northeastern margin of the Caetano caldera. (A) Large block of Devonian Slaven Chert (Dsc) in white Caetano Tuff (Tcl) near northeastern caldera margin in northern Toiyabe Range. Low rocky ridge is Slaven Chert in caldera margin at A (Fig. 15); caldera boundary fault is developed in the chert. View looking north. (B) Steep caldera structural margin at B (Fig. 15). View looking west-northwest. (C) Close-up view of steep caldera structural margin at B (Figs. 15 and 16B). Densely welded, highly stretched Caetano Tuff is in sharp, approximately vertical contact with brecciated and recemented Devonian Slaven Chert outside caldera. (D) Caldera topographic wall at C (Fig. 15), showing megabreccia consisting of multiple blocks of Devonian Slaven Chert up to at least 50 m in diameter, locally with thin lenses of Caetano Tuff. Light-colored middle ground is lithic-rich Caetano Tuff containing clasts of chert and 35 Ma rhyolite, which crops out just to the right of the photo as megabreccia. View looking west-northwest.

Figure 17. Photographs showing breccias and conglomerate in the Caetano caldera. (A) Large clast of brecciated, Paleozoic quartzite in lithic-rich layer in Caetano Tuff on east side of Toiyabe Range. Layer previously was mapped as conglomerate bed within the Caetano Tuff by Gilluly and Masursky (1965). (B) Mesobreccia sheet in Caetano Tuff on the southwest side of Carico Lake Valley. Mesobreccia composed of angular clasts of siliceous siltstone, quartzite, chert, and chert-pebble conglomerate up to 70 cm in diameter in a more finely clastic, non-tuffaceous matrix. Lens extends several hundred meters along strike. Hammer is 46 cm long. (C) Limestone clasts in Tertiary conglomerate underlying caldera floor near Wenban Spring, Toiyabe Range. (D) Hydrothermally brecciated Redrock Canyon pluton in low hills northwest of Carico Lake. Matrix-supported breccia consists of clasts of Redrock Canyon pluton pervasively altered to kaolinite + quartz in matrix of quartz, Fe-oxide minerals (mostly hematite), and local barite. Note larger brecciated clast in bottom of photo that has hydrothermal matrix filling fracture.

in Paleozoic rock. However, the four shown on Figure 15 are mostly to entirely surrounded by Caetano Tuff, and clasts of the rhyolite are common in adjacent lithic-rich tuff. As with the chert megabreccia, several of the rhyolite blocks are probably composite.

Gilluly and Masursky (1965) mapped megabreccia and some mesobreccia as in-place Paleozoic Valmy Formation or Slaven Chert, depending on whether the blocks were quartzite or chert, or rhyolite dikes and other mesobreccia lenses as Tertiary conglomerate. However, the large size of clasts and their interbedding or interfingering with Caetano Tuff demonstrates that they are megabreccia and mesobreccia. The distinctive clast types are consistent with outcrops in the caldera wall north of the Copper Fault and in the Cortez Range to the east. We also found limestone clasts that are probably derived from lower plate Wenban Formation, which crops out below Tertiary gravel in the Cortez Range. Lower plate rocks are recognized in breccia only in the eastern part of the caldera. Rhyolite clasts are petrographically identical to the ca. 35 Ma rhyolite dikes in the Cortez Mine and a small rhyolite dome in the Cortez Range (Plate 1). The large, east-striking body at C (Fig. 15), which is probably composite, is one of the rhyolites dated by Wells et al. (1971).

Other Mesobreccia and Megabreccia Locations

Massive to layered mesobreccia or megabreccia crops out near the caldera margin in many locations. A notable occurrence is just west of Carico Lake Valley (Plate 1). Mesobreccia composed of angular clasts of siliceous siltstone, quartzite, chert, and chert-pebble conglomerate up to 70 cm in diameter in a more finely clastic, non-tuffaceous matrix is interbedded with probably uppermost Caetano Tuff. Irregular bedding is defined by variations in clast type, size, and abundance (Fig. 17B). The mesobreccia layers form several thick sequences with minor interbedded Caetano Tuff; the entire mesobreccia sequence is at least 100 m thick.

Although most breccia is within 1–2 km of the caldera margin, at least one occurrence is more than 4 km from the nearest margin. Mesobreccia that crops out within the upper Caetano Tuff unit northeast of Red Mountain near Tub Spring (Plate 1) is the most distant from the caldera margin that we found. The breccia in this area contains blocks of chert up to 5 m long (Fig. 13D). This breccia was deposited very late during eruption and caldera collapse. The caldera margin may have had its greatest relief so that breccia could travel the farthest from the margin.

Upper Unit of Caetano Tuff near Tub Spring

The character of the upper unit of Caetano Tuff is best illustrated northwest of Tub Spring in the south-central part of the caldera, where the lower-upper contact is repeated by several northwest-striking, down-to-the-southwest faults (Plate 1; Fig. 8C). The simple, lower unit is composed of dark, densely welded tuff that forms few separable ledges and is locally capped by a dark vitrophyre. The composite upper unit is commonly light-colored to banded on air photos, with repeated poorly to densely welded sections and common sedimentary interbeds.

The base of the upper unit is marked variably by a vitrophyre or vitrophyre breccia presumably reworked from the lower unit or a clay-rich zone probably marking weathered formerly glassy, poorly welded tuff or tuffaceous sediment. This soft zone forms a distinct topographic break. At one location, vitrophyre breccia is overlain by a probable debris-flow deposit composed of angular blocks of devitrified Caetano Tuff up to 2 m in diameter. The breccia is overlain by well-bedded tuffaceous to pebbly coarse sandstone with abundant pumice, quartz, sanidine, quartzite, and chert up to 4 mm in diameter.

The rest of the upper unit consists of repeated, poorly welded, or zoned poorly to moderately to rarely densely welded tuffs that commonly contain abundant lithic fragments. Subangular fragments of densely to poorly welded Caetano Tuff up to 1.4 m in diameter are most common (Fig. 8D), but some tuffs are dominated by hornblende-pyroxene andesite and Paleozoic fragments up to 15 cm. Poorly to moderately welded tuff characterized by distinctive orange pumice fragments are common and locally interbedded with dark, densely welded tuff. "Orange-pumice tuff" is present in most other areas of the upper unit. Sedimentary interbeds of varied thickness separate the tuffs or sequences of tuffs. These deposits range from coarse conglomerate or debris flows to fine, platy tuffaceous siltstone. Conglomerates commonly consist of a lag of angular to subrounded Caetano Tuff up to 1 m in diameter or chert pebbles and cobbles in a clayey soil. Well-bedded coarse sandstone is common.

The change from lower to upper unit probably marks an abrupt change in eruption dynamics, from continuous to more sporadic eruption near the end of the caldera cycle. The more sporadic eruptions allowed greater cooling zonation and time for sediment deposition between ash flows. The sedimentary interbeds probably are laterally equivalent to the thick, upper mesobreccias and megabreccias near the caldera margin at Red Mountain. Rock fall or rock avalanche deposits spalled from the margin probably were reworked into debris-flow or fluvial deposits farther from the margin.

Caldera Floor at Caetano Ranch

The caldera floor is exposed for ~4 km along strike in the footwall of the Caetano Ranch fault in the southeastern part of the caldera (Plate 1, Fig. 18). In this area, more than 3 km of intracaldera Caetano Tuff overlies Tertiary andesite and conglomerate and Paleozoic quartzite, limestone, and chert-quartzite-pebble conglomerate. Paleozoic limestone and conglomerate crop out together in a large area in the footwall of the Caetano Ranch fault. The conglomerate has well-rounded pebbles up to 5 cm in diameter in a well-cemented, red-weathering, presumably ferruginous matrix (Fig. 4A). It is faintly to well bedded, strikes east, and dips variably north and south. The massive limestone did not yield conodonts (A.G. Harris, 2007, written commun.), but we infer that it and conglomerate are probably part of the Pennsylvanian-Permian Antler sequence, which crops out in several areas south and northeast of the Caetano caldera, including in the Cortez Range ~20 km to the northeast (Gilluly and Masursky, 1965) and The Cedars area (Moore et al., 2000). Quartzite, which crops out north of the area shown in Figure 18, is probably part of the Valmy Formation in the upper plate of the Roberts Mountains thrust (Gilluly and Masursky, 1965).

Tertiary conglomerate crops out beneath the caldera fill in the southern part of Figure 18. It dips ~40° east, together with the overlying andesite and Caetano Tuff, consistent with no deformation between deposition of the gravel and eruption of tuff. The gravel is faulted against Caetano Tuff and post-tuff sedimentary rocks to the west. The conglomerate contains angular to moderately rounded clasts of limestone to 70-cm-long and lesser chert and quartzite in a calcite-cemented matrix (Fig. 17C). Conodonts from a limestone clast are long-ranging morphotypes that span the Silurian to the Mississippian (A.G. Harris, 2007, written commun.) and are consistent with Lower Paleozoic limestone from the lower plate of the Roberts Mountains allochthon, probably the Devonian Wenban Limestone exposed in the nearby Cortez Range. The lithologic and structural differences demonstrate that this conglomerate is not the same unit as the Paleozoic conglomerate.

Finely porphyritic, andesite lava containing plagioclase, pyroxene, and lesser hornblende phenocrysts overlies pre-volcanic conglomerate or Paleozoic rocks. The andesite reaches a maximum thickness of 300–400 m where it overlies limestone and chert-quartzite-pebble conglomerate and thins to the north and south.

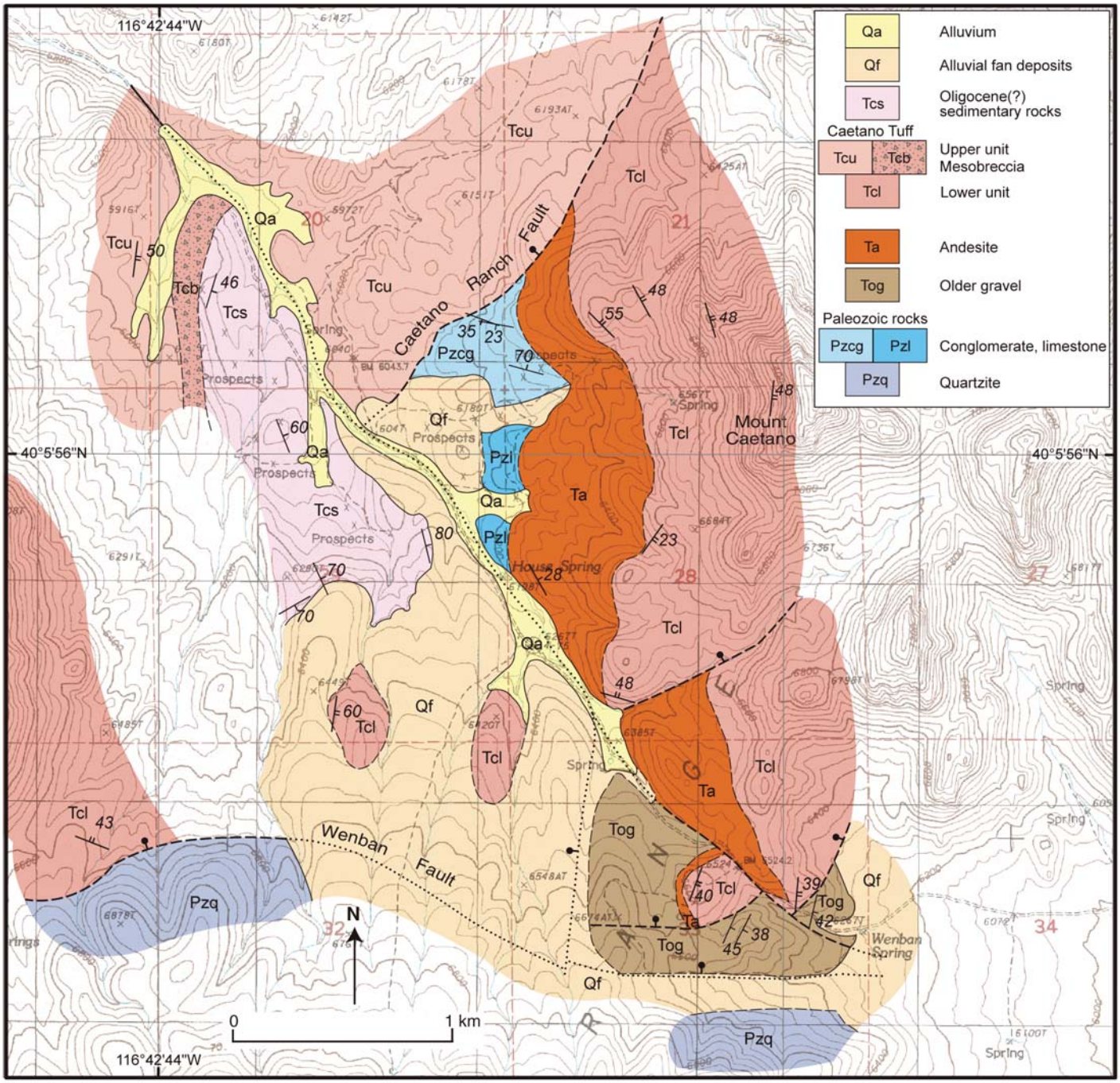

Figure 18. Geologic map of the caldera floor and intracaldera Caetano Tuff near Caetano Ranch (Wenban Spring 7-½' quadrangle). The caldera floor, which is exposed for ~4 km along strike, consists of Permian-Pennsylvanian Antler overlap sequence limestone and conglomerate (Fig. 4A), overlain by andesite lavas. The lower unit of intracaldera Caetano Tuff, as much as 3.6 km thick, overlies the pre-caldera rocks. The upper unit of Caetano Tuff including mesobreccia crops out on the downthrown side of the middle Miocene Caetano Ranch Fault. Paleozoic Valmy Formation south of the Wenban Fault constitutes the southern caldera wall.

Approximately 15 m of andesite separates pre-volcanic conglomerate from Caetano Tuff in the south. Just north of Figure 18, a thin layer of andesite appears to have filled in and smoothed over irregular topography on Valmy quartzite (Plate 1).

The Caetano Tuff in the Toiyabe Range has a basal vitrophyre and also has several intratuff vitrophyres, an unusual feature for a thick intracaldera tuff. In other respects, it is similar to Caetano Tuff throughout the caldera. For example, Mount Caetano consists of more than 1000 m of monotonous, densely welded, devitrified ash-flow tuff (Fig. 7A). In contrast, the upper Caetano Tuff, which is well preserved on the downthrown side of the Caetano Ranch Fault, varies from densely to poorly welded and devitrified to glassy. This suggests more sporadic

eruptions during the waning stages of Caetano eruption. Mesobreccia with clasts of Caetano Tuff, andesite, quartzite, chert-quartzite-pebble conglomerate, and marble up to 2.5 m in diameter overlie the upper unit tuff. Fine, tuffaceous sedimentary rocks that may be moat sediments overlie the mesobreccia.

Resurgent Intrusion

The Carico Lake pluton, a granite porphyry similar in phenocryst assemblage, composition, and age to Caetano Tuff, crops out in a series of low hills surrounded by Quaternary deposits in Carico Lake Valley (Plate 1) and probably underlies an area of at least 25 km^2. The intrusion is distinguished from surrounding tuff by being generally massive and locally flow banded (Fig. 7D), by lacking ash-flow tuff features such as pumice, by being more coarsely porphyritic with phenocrysts of sanidine to 2 cm, and by having a fine-grained, holocrystalline groundmass. Although the contact with tuff is nowhere exposed, field relations along part of the southern margin of the intrusion show that the granite intruded, domed, and brecciated the surrounding Caetano Tuff (Fig. 19).

The Carico Lake pluton crops out at the north end of irregular ridges east of Carico Lake and in several low hills to the northeast (Fig. 19). The southern and western parts of the ridges consist of Caetano Tuff that strikes anomalously east and has a near vertical dip. In the northern and eastern parts of the ridge, Caetano Tuff is overlain by a breccia composed of angular clasts of Caetano Tuff up to at least 5 m in diameter in a matrix of finely ground tuff. The breccia is overlain by clastic sedimentary rocks and the 30.5 Ma "B" and 28.8 Ma "C" units of the Bates Mountain Tuff (Table 1), which, unlike the underlying Caetano Tuff, have typical north strikes and moderate east dips (Fig. 19).

We interpret these relations to indicate that the pluton domed the Caetano Tuff, generating the anomalous east strike and steep dips. Removing tilting from middle Miocene extension would not significantly change the anomalous strikes, because Miocene extensional tilting was approximately parallel to the anomalous strike. The breccia resulted from gravitational sliding of steeply tilted and uplifted Caetano Tuff over the dome. Similar breccia is recognized around ca. 24 Ma felsic domes in western Nevada (Faulds et al., 2003; Henry et al., 2004). The overlying, undomed sedimentary rocks and ash-flow tuff then filled in over and around the dome and breccia. Intrusion, doming, and brecciation probably occurred within ca. 100,000 yr of ash-flow eruption and caldera collapse, given the indistinguishable ages of the intrusion and the Caetano Tuff, and had to have occurred before 30.5 Ma, the age of the "B" unit of Bates Mountain Tuff.

Pre-Caldera Paleovalley

Pre-Caetano Tuff sedimentary and volcanic deposits crop out east (southwestern Cortez Range) and west (east side of the Fish Creek Mountains) of the caldera, and underlie the caldera floor in the northern Toiyabe Range (Plate

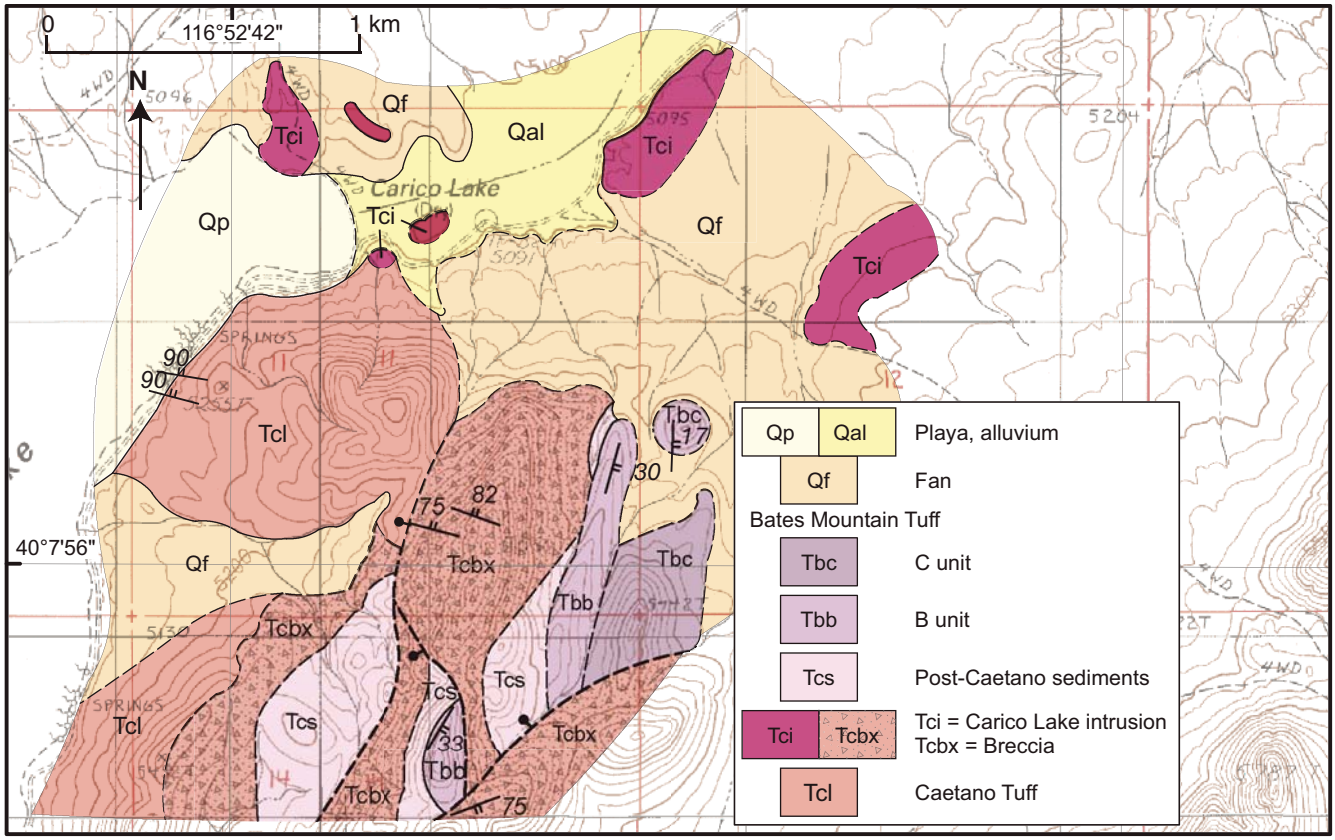

Figure 19. Geologic map of Carico Lake pluton, a resurgent intrusion of granite porphyry that intruded and steeply tilted Caetano Tuff near the middle of the caldera (Carico Lake North and Rocky Pass 7-½' quadrangles). A breccia composed of coarse blocks of Caetano Tuff (Tcbx) probably formed by gravitational sliding of steeply tilted and uplifted tuff over the intrusion. The B and C units of the Bates Mountain Tuff show the normal, moderate, east dip resulting from middle Miocene extension (Colgan et al., 2008.

1). Thin Tertiary basalt flows overlain by the tuff of Cove Mine form the caldera floor southwest of Wilson Pass and probably filled pre-caldera paleotopography (Fig. 14). We infer that these sedimentary and volcanic rocks were deposited in a west-trending paleovalley that may have been laterally continuous with the Golconda Canyon paleovalley 40 km to the west in the Tobin Range (Fig. 2; Gonsior, 2006; Gonsior and Dilles, 2008). The base of the Golconda Canyon paleovalley also was filled with Tertiary basalt flows that were, in turn, overlain by as much as 250 m of outflow Caetano Tuff, while the eastern part of the paleovalley was buried when the caldera collapsed.

In the southwestern Cortez Range, a thick sequence of poorly exposed gravel overlies both upper and lower plate rocks of the Roberts Mountains allochthon and is overlain by middle Miocene basaltic andesite flows (Plate 1; Gilluly and Masursky, 1965; Stewart and Carlson, 1976). These poorly sorted and poorly lithified deposits are ≥400 m thick and contain blocks of both upper and lower plate Paleozoic rocks, granitic rocks, porphyritic andesites, flow-banded rhyolites, Caetano Tuff, and younger tuffs including units A(?), B, and D of the Bates Mountain Tuff. Blocks in the gravels are as much as 10 m across, and concentrations of monolithologic blocks form hilltops and ridgelines as much as 200 m long. The presence of clasts of unit D of the Bates Mountain Tuff indicates a maximum age of ca. 25.3 Ma for parts of these deposits. However, sanidine phenocrysts from a waterlain, air-fall tuff yielded an $^{40}Ar/^{39}Ar$ age of 33.97 ± 0.20 Ma (Table 1), suggesting that parts of the gravels are at least this old. We interpret this tuff as an ash fall related to eruption of the Caetano Tuff and infer that these gravels were deposited in a long-lived paleovalley that had been incised into the lower plate of the Roberts Mountains allochthon prior to eruption of the Caetano Tuff.

Tertiary conglomerates that underlie the Caetano caldera are exposed on both sides of the northern Toiyabe Range (Plate 1). Several hundred meters of strongly lithified calcareous sandstone and pebbly conglomerate containing abundant Paleozoic limestone clasts crop out near Wenban Spring (see description of Caldera floor at Caetano Ranch). Poorly exposed, locally well-lithified conglomerate also underlies intracaldera Caetano Tuff on the northwestern edge of the Toiyabe Range. This conglomerate contains subrounded clasts of quartzite, chert, argillite, granite, diorite, and several textural types of rhyolite as much as 1.5 m in diameter in a sandy noncalcareous matrix (Fig. 4B).

Tuffaceous sedimentary rocks interbedded with andesite and dacite flows form the basal Tertiary deposits and underlie outflow Caetano Tuff in Horseshoe Basin on the northeast side of the Fish Creek Mountains (Fig. 2; Stewart and McKee, 1977).

We interpret that these pre-Caetano Tuff sedimentary and volcanic deposits filled a paleovalley at least 400 m deep that drained west from the southern Cortez Range across the Tobin Range (Fig. 2). Most of the paleovalley corresponds to the volcano-tectonic trough of Masursky (1960) and Burke and McKee (1979). However, our interpretation of the origin of this paleovalley differs from previous workers, as discussed in a later section. The paleovalley was disrupted by formation of the Caetano and Fish Creek Mountains calderas, although sediments and tuffs continued to be deposited within the Caetano caldera throughout the lifetime of the paleovalley as shown by the ages of tuffs deposited in the Caetano caldera and in Golconda Canyon and present as clasts in the gravels in the Cortez Range. Unit D of the Bates Mountain Tuff at 25.27 Ma is the youngest recognizable clast in the gravel deposits in the Cortez Range and youngest tuff inside the Caetano caldera, and drainage across the Caetano caldera may have been permanently disrupted by formation of the Fish Creek Mountains caldera at 24.72 Ma (Table 1; McKee, 1970).

Hydrothermal Alteration in the Caetano Caldera

Intracaldera Caetano Tuff is hydrothermally altered along the entire north-south extent of the caldera from Elephant Head north to Wilson Pass, and along the southern caldera margin from the Shoshone Range to southwest Crescent Valley (Plate 1). Alteration of the Caetano Tuff generally is absent on the north side of Carico Lake Valley, at Rocky Pass, and in the northern Toiyabe Range. The Carico Lake pluton is unaltered to very weakly altered and forms the northeast boundary of alteration. In contrast, the Redrock Canyon pluton is pervasively altered.

Three major, hydrothermal alteration assemblages are recognized: (1) vuggy silica, (2) advanced argillic, and (3) intermediate argillic. In vuggy silica alteration, both plagioclase and K-feldspar phenocrysts are leached leaving prominent voids, and the groundmass is replaced by fine-grained silica with several percent disseminated, fine-grained pyrite that is mostly oxidized. Vuggy silica alteration is transitional to advanced argillic alteration that consists of a kaolinite-quartz ± pyrite assemblage in which both plagioclase and sanidine phenocrysts are replaced by kaolinite, biotite is altered to kaolinite or opaque oxide minerals, and the groundmass is replaced by kaolinite and fine-grained silica. Minor alunite is present locally. Most advanced argillic alteration is oxidized, but relict, disseminated, fine-grained pyrite is present locally. In many rocks, abundant hematite is present. Advanced argillic alteration is transitional to intermediate argillic alteration in which fine-grained kaolinite replaces plagioclase phenocrysts, and sanidine phenocrysts are generally unaltered or are perthitic. Biotite phenocrysts are variably replaced by opaque oxides, white mica, or are relatively unaltered. Groundmass is altered to a mixture of fine-grained silica and kaolinite. Narrow (<5-cm-wide) quartz ± pyrite veins are present locally in zones of vuggy silica and advanced argillic alteration, notably along the south margin of the caldera on both sides of Carico Lake Valley, and thin sedimentary beds are locally silicified in the upper Caetano unit (Fig. 8B), but no major zones of quartz veining or silicification were recognized. Hydrothermal breccias cemented with quartz, Fe-oxides, and barite were recognized in the Redrock Canyon pluton on the northwest side of Carico Lake (Fig. 17D). In general, alteration is most intense along the south caldera margin on both sides of Carico Lake Valley, and in the west-central part of the caldera in and around the Redrock Canyon pluton between Redrock Canyon and Carico Lake Valley (Plate 1).

Although strong hydrothermal alteration affects intracaldera Caetano Tuff, overlying sedimentary rocks and the Bates Mountain Tuff are unaltered. The Redrock Canyon pluton is strongly altered to argillic and advanced argillic assemblages similar to alteration in the surrounding Caetano Tuff. In contrast, the Carico Lake pluton is unaltered, intracaldera Caetano Tuff along the north and east sides of the pluton are generally unaltered and locally vitrophyric, and altered Caetano Tuff is generally absent farther east inside the caldera. These relations suggest that hydrothermal alteration of the Caetano caldera is related to emplacement of the Redrock Canyon pluton in the west-central part of the caldera shortly after eruption of the Caetano Tuff and caldera collapse. We infer that emplacement of the Carico Lake pluton postdates alteration.

Widespread, advanced argillic alteration, such as in the Caetano caldera, is uncommon in ash-flow calderas elsewhere, where propylitic and/or argillic alteration are more typical (e.g., Lipman, 1984; John and Pickthorn, 1996). Alteration in the Caetano caldera more closely resembles shallow magmatic-hydrothermal alteration in porphyry systems formed by degassing of shallowly emplaced, sulfur-rich magmas, although the presence of hypogene(?) hematite and only sparse alunite suggests that the Caetano hydrothermal fluids were relatively sulfur poor. We attribute the abundance of advanced argillic alteration in the Caetano caldera to the very shallow emplacement (<1 km) of the Redrock Canyon pluton into water-saturated, interbedded

poorly welded tuff and sedimentary rocks of the upper Caetano Tuff unit. The large volume of altered rock likely indicates that the entire west half of the Caetano caldera is underlain by intrusive rocks at shallow depths.

DISCUSSION

Distribution, Volume, and Source of the Caetano Tuff and Tuff of Cove Mine

Petrologic, geochemical, and geochronologic data presented above show that the previously identified Caetano Tuff consists of two distinct ash-flow tuffs, the ca. 33.8 Ma Caetano Tuff and the older (ca. 34.2 Ma), more mafic tuff of Cove Mine. The spatial distribution of these tuffs is shown in Figure 2. The tuff of Cove Mine is limited to scattered exposures on the north side of the Caetano caldera that extend ~40 km north from the caldera to just south of the town of Battle Mountain. Most of the Caetano Tuff is exposed within the structurally dismembered Caetano caldera, but outflow tuff from the caldera is exposed in the Tobin Range, 40 km west of the caldera and in the Toiyabe Range near Cowboy Rest Creek, ~30 km south of the caldera (Fig. 1). Coarse blocks of Caetano Tuff also are present in the gravel deposits immediately east of the caldera in the southwestern Cortez Range, although no outflow Caetano Tuff has been found east of the caldera.

The volume of intracaldera Caetano Tuff is crudely estimated at ≥840 km^3 using a restored area of ~280 km^2 for the outline of the caldera after removing 100% post-caldera extension (Colgan et al., 2008) and an average thickness of 3 km for intracaldera Caetano Tuff. Intracaldera tuff thickness is based on an exposed thickness of >3.4 km in the northeast part of the caldera and ~2.0 km for the northwest part of the caldera. The volume of preserved extracaldera Caetano Tuff to the south and west sides of the caldera is difficult to estimate but is probably small. However, the 1 km excess of collapse over intracaldera tuff suggests that an additional ~280 km^3 probably erupted as outflow tuff that was subsequently eroded or as widely dispersed pyroclastic-fall tuff. Therefore, a conservative minimum estimate of the total erupted volume of Caetano Tuff is ~1100 km^3.

The source of the Caetano Tuff has long been inferred to be in the northern Toiyabe Range or Shoshone Range, which have been variably described as a volcano-tectonic trough or depression (Masursky, 1960; Gilluly and Masursky, 1965; Stewart and McKee, 1977; Burke and McKee, 1979) or as one (Best et al., 1989; McKee and Moring, 1996) or two (Ludington et al., 1996) calderas on small-scale regional maps. As demonstrated by the distribution of the Caetano Tuff, the great thickness of intracaldera tuff, and the presence of cogenetic age-equivalent intrusions in the center of the caldera, our study conclusively proves that the Caetano caldera is the source of the Caetano Tuff.

The source of the tuff of Cove Mine is unknown but seems likely to be within its known distribution. It is thickest in the northern Fish Creek Mountains, suggesting a source may be buried beneath the ca. 24.7 Ma Fish Creek Mountains caldera or beneath younger sediment in a nearby valley. Burial beneath the Caetano caldera is precluded by absence of the tuff of Cove Mine in exposures of the caldera floor in the Toiyabe Range and by its presence only as a thin (50–100 m) outflow sheet on the caldera floor at Wilson Pass.

Wrucke and Silberman (1975) proposed a caldera at Mount Lewis for the entire Caetano Tuff at a time when the tuff's dual nature and source were not recognized (Fig. 2). However, even the existence of a caldera at this location is highly controversial (Gilluly, 1977; Wrucke and Silberman, 1977). Wrucke and Silberman (1975) cite numerous K-Ar ages that show that volcanic and intrusive rocks within their proposed caldera are similar in age to the Caetano Tuff. However, most outcrop within the proposed caldera consists of Paleozoic rocks, and the Caetano Tuff is absent within the caldera. This requires that any intracaldera Caetano Tuff be completely eroded, leaving only numerous, small intrusions and odd, locally derived volcanic breccias. No other known or proposed caldera in Nevada has been completely stripped of its intracaldera tuff (Best et al., 1989; Boden, 1992; John, 1995; Henry et al., 1999). Thus, the source of the tuff of Cove Mine remains unknown.

Caetano Caldera Evolution

Miocene extensional faulting and tilting has exposed the interior of the Caetano caldera over a paleodepth range of >5 km, from beneath the caldera floor through post-caldera sediments, providing constraints on an evolutionary model of the Caetano caldera that are rarely available for other calderas (Fig. 20). In this paper, we present a model for the formation of the Caetano caldera that is based on the extensive field observations and analytical data discussed in earlier sections.

The Caetano caldera formed over an area of relatively low relief developed on Paleozoic rocks and incised by a broad, west-trending paleovalley locally filled with at least 400 m of gravel and conglomerate (Fig. 20A). The lack of pre-Caetano faults, angular unconformities, or sedimentary basins are consistent with the region not undergoing extension before the middle Miocene (Colgan et al., 2008). The presence of lower-plate limestone clasts in strongly lithified, pre-Caetano Tuff conglomerate in the Toiyabe Range indicates that the paleovalley had cut down through the <1-km-thick, upper plate of the Roberts Mountains allochthon prior to eruption of the Caetano Tuff.

Volcanic activity in the area immediately preceding formation of the Caetano caldera was minor; the caldera did not form over a precursor volcano. Rhyolite dikes and small domes exposed near the northeast margin of the caldera (Gilluly and Masursky, 1965) are ca. 1.5 Ma older than the caldera (Wells et al., 1971; Mortensen et al., 2000) but might represent early activity related to the caldera-forming magma. A large rhyolite center is exposed in the Simpson Park Range, ~12 km southeast of the caldera (volcanics of Fye Canyon; Gilluly and Masursky, 1965), but these silicic lavas also are ca. 1–1.5 Ma older than the Caetano caldera (K-Ar ages of 34.8 ± 1.0 and 35.4 ± 1.0 Ma; McKee and Conrad, 1994). Thin, undated andesite/basalt flows fill local topographic depressions below the caldera floor in the northern Toiyabe Range and west of Wilson Pass in the Shoshone Range, and more extensive andesite/dacite flows are interbedded with sedimentary rocks west of the caldera on the east side of the Fish Creek Mountains. The sources of these lavas are unknown. Outflow tuff of Cove Mine locally filled paleotopography, mostly north of the Caetano caldera, and locally overlies thin basalt flows southwest of Wilson Pass within the caldera.

Formation of the Caetano caldera began with eruption of the lower unit of the Caetano Tuff and collapse along steep, caldera-bounding faults at ca. 33.8 Ma (Fig. 20B). Outflow Caetano Tuff flowed primarily to the west and south of the caldera, locally filling the west-trending paleovalley that drained the area overlying the caldera. The lower unit of intracaldera Caetano Tuff apparently forms a single, compound cooling unit as much as 3600 m thick. A prominent 10- to 20-m-thick basal vitrophyre is preserved in the eastern part of the caldera that was not affected by hydrothermal alteration. Several other vitrophyric layers are preserved in the northern Toiyabe Range; these vitrophyres represent quench zones around lithic-rich layers within the tuff rather than marking cooling breaks between ash flows. The lower unit is normally zoned compositionally from high-silica rhyolite at the base to low-silica rhyolite at the top.

Caldera collapse was asymmetric, with greater amounts of collapse and thicker caldera fill in the eastern part of the caldera. Total collapse was as much as 5 km in the eastern part

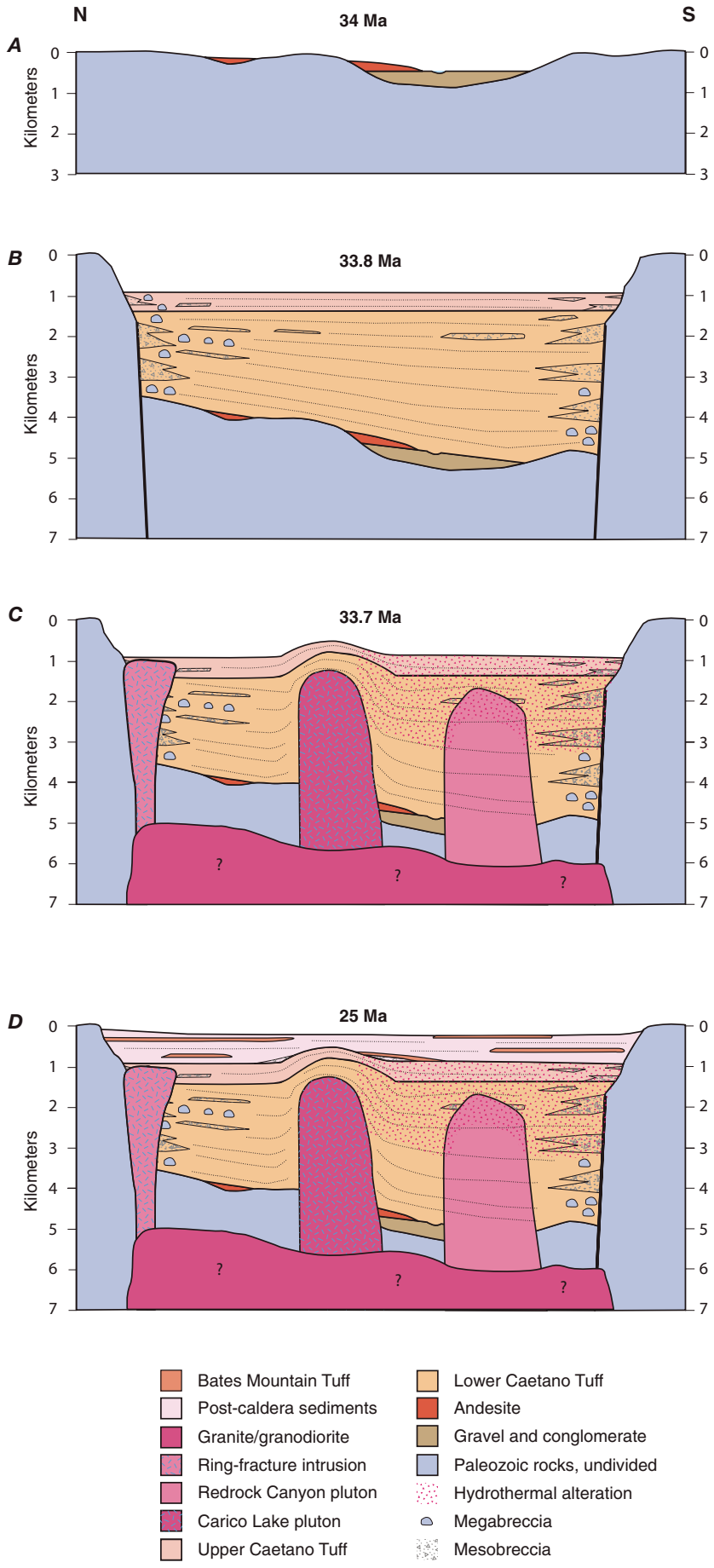

Figure 20. Cartoon model showing evolution of the Caetano caldera. Sections are ~N-S through the center of the caldera. No vertical exaggeration. (A) ca. 34 Ma shortly before caldera formation. Caldera site underlain by irregular erosional surface on Paleozoic rocks locally cut by Tertiary paleovalleys, partly filled with gravels and andesite lava flows. (B) 33.8 Ma following eruption of the thick lower unit of Caetano Tuff, caldera collapse with megabreccia blocks and mesobreccia lenses shed into the caldera, and eruption of the much thinner upper unit of Caetano Tuff. Caldera collapse was significantly greater in the eastern part of the caldera than in the western part. (C) 33.7 Ma following intrusion of the Carico Lake and Redrock Canyon plutons, resurgent doming around Carico Lake pluton, shedding of breccias off the resurgent dome, circulation of hydrothermal fluids and extensive hydrothermal alteration in western part of caldera probably related to the Redrock Canyon intrusion, and emplacement of small, ring-fracture intrusion; (D) 25.3 Ma following a long period of deposition of sediments and distal outflow tuffs (mostly Bates Mountain Tuffs) in caldera depression. Early sediments may have been lacustrine and deposited in a moat around the resurgent dome. Later sediments are mostly fluvial.

of the caldera but only ~3.0–3.5 km in the northwestern part. The caldera-bounding faults dipped vertically to steeply inward, although exposed caldera margins likely were modified to shallower dips by slumping. The caldera floor was nearly flat, as shown by more than 6 km of along-strike exposure in several fault blocks in the northern Toiyabe Range. The coherence of caldera floor and the regular compaction of Caetano Tuff throughout the caldera indicate that collapse was by piston-like subsidence (Lipman, 1997). Numerous blocks of megabreccia and beds and lenses of mesobreccia were shed into the caldera from adjacent walls and commonly extend 1–2 km into the caldera.

Eruption of the upper unit of the Caetano Tuff, also at ca. 33.8 Ma, followed a complete cooling break and local deposition of thin beds of siltstone and sandstone. Multiple, thin cooling units of ash-flow tuff interbedded with thin sedimentary units that total as much as 1000 m in thickness comprise the upper unit of the Caetano Tuff. These tuffs commonly are poorly welded, locally contain thin (5- to 10-m-thick), densely welded vitrophyre zones, and commonly have undergone vapor-phase alteration. Lithic-rich beds are common and contain both pre-caldera wall rocks and blocks of densely welded, lower Caetano Tuff. Slowing of ash-flow eruption and development of complex intracaldera stratigraphy are common features during the waning stages of the caldera cycle (Smith and Bailey, 1968; Boden, 1986).

Emplacement of several shallow, granite porphyry intrusions in the central and western parts of the caldera closely followed eruption of the upper unit of Caetano Tuff (Fig. 20C). Three intrusions are exposed: the unaltered, 25-km^2 Carico Lake pluton and a small, ring-fracture intrusion in Carico Lake Valley and the altered Redrock Canyon pluton. Compositions of the unaltered intrusions suggest that they are slightly more mafic, residual magma of the magma that erupted to form the Caetano Tuff. These resurgent intrusions rose within a few hundred meters of the paleosurface and locally domed and steeply tilted, intracaldera, Caetano Tuff. Sanidine $^{40}Ar/^{39}Ar$ ages show that eruption of the Caetano Tuff, magma resurgence, and emplacement of these intrusions spanned no more than ca. 100,000 yr. The intrusions probably coalesce at depth beneath the western part of the caldera similar to exposures of deeply eroded calderas and underlying plutons elsewhere (e.g., Lipman, 1984, 2007). The Caetano caldera, with only one ring-fracture intrusion, is unlike many calderas that have abundant ring-fracture intrusions or lava domes (Smith and Bailey, 1968; Lipman, 1984; Boden, 1986).

The Redrock Canyon intrusion and adjacent upper and lower units of the Caetano Tuff are strongly hydrothermally altered, and we infer that convective circulation of the hydrothermal fluids responsible for the alteration likely was driven by the Redrock Canyon intrusion. Alteration extended to paleodepths of >1.5 km but was most intense at shallower depths, such as in the upper unit of Caetano Tuff adjacent to the Redrock Canyon pluton and along the south caldera margin on both sides of Carico Lake Valley. Although not preserved, hot springs likely were associated with the hydrothermal system.

Total caldera collapse of as much as 5 km exceeded the thickness of intracaldera tuff by at least 1 km, leaving a deep depression that acted as a depocenter for sediments and distally erupted tuffs for the next ca. 10 Ma (Fig. 20D). The center of the caldera was domed by the resurgent intrusions, and a lake formed in the deepest parts of the depression, notably on the east and west sides of the caldera. Early sediments deposited in the caldera include breccias containing hydrothermally altered tuff derived from the domed central part of the caldera and fine-grained moat sediments along the outer margins of the caldera. The lake apparently was short lived, however, as most of the sediments filling the caldera depression are coarser grained fluvial deposits. The change from lacustrine to fluvial sedimentation might mark reestablishment of westward drainage across the caldera and breaching of the caldera walls. Units B, C, and D of the Bates Mountain Tuff were deposited in the caldera, interbedded with the fluvial sediments, thereby showing that sedimentation of the caldera depression continued until at least 25.3 Ma and possibly somewhat later.

Implications of the Caldera Origin of the Caetano Tuff and Volcano-Tectonic Troughs

Recognition that the Caetano caldera is not part of a long-lived, west-elongated volcano-tectonic trough has important implications for the Cenozoic tectonic history of northern Nevada. The Caetano caldera was previously interpreted as the northern of two volcano-tectonic troughs in Nevada (Fig. 1; Masursky, 1960; Burke and McKee, 1979), and the presence of these east-west elongated features seemingly requires significant and prolonged, middle Tertiary, north-south extension. Many features characteristic of ash-flow calderas, however, also may be characteristic of volcano-tectonic troughs or depressions (Table 2).

A key distinction between volcano-tectonic troughs and ash-flow calderas is that the former are highly elongate and the latter are generally more equant, and almost no calderas have length-to-width ratios greater than two (Newhall and Dzurisin, 1988). Masursky (1960) and Burke and McKee (1979) interpreted the Caetano trough to be more than 90 km long, east-west, and 10–25 km wide, north-south. However, this great length results from combining the Caetano caldera with the much younger and unrelated, Fish Creek Mountains caldera and with the paleovalley in the Tobin Range (McKee, 1970; Gonsior, 2006; Fig. 2). The remaining ~40-km east-west dimension of the Caetano caldera reflects ~100% east-west extension in the middle Miocene (Colgan et al., 2008). Before Miocene extension, we propose that the caldera was trapezoidal in shape and ~20 km long and 10–18 km wide.

Unlike ash-flow calderas that form instantaneously on geologic timescales, volcano-tectonic troughs are potentially long-lived features that may take millions of years to form (Table 2) and accumulate interbedded ash-flow tuffs, sedimentary rocks, and lava flows of significantly different ages. For example, an "intra-arc half graben" in the Challis volcanic field developed over ca. 3 Ma and was filled by a complex sequence of at least five ash-flow tuffs and interbedded sedimentary rocks and lavas (Janecke et al., 1997). In contrast, the Caetano caldera collapsed nearly instantaneously, forming a semi-equant depression mostly filled with >3 km of Caetano Tuff. No lavas are interbedded with Caetano Tuff, and the only significant sedimentary deposits are megabreccias and mesobreccias, which also accumulate nearly instantaneously during caldera collapse, and thin sedimentary rocks interbedded in the upper unit. Post-Caetano caldera sediments and tuffs accumulated in the depression left by caldera collapse for 8–9 Ma, but there is no evidence that the caldera underwent additional volcanic or tectonic subsidence during this time.

The key tectonic difference between a caldera and a "volcano-tectonic trough" is that caldera collapse is a localized phenomenon caused by evacuation of the underlying magma chamber, whereas trough subsidence is the result of far-field extensional stress causing a fault-bounded graben or half graben to form. An east-west elongate, fault-controlled Caetano trough would thus require significant north-south extension in the middle Tertiary. The study area did undergo significant E-W extension during the middle Miocene, but we have found no evidence for north-south extension at any time (Colgan et al., 2008). Although not called upon by Masursky (1960) or Burke and McKee (1979), several other geologists have suggested north-south extension accompanied Cenozoic magmatism in the Great Basin (e.g., Speed and Cogbill, 1979; Best, 1988; Bartley, 1989; Bartley et al., 1992). In some cases, other explanations are

available for the interpreted north-south extension. For example, Rowley (1998) discussed several zones of generally east-west structures and igneous belts but attributed them to reactivation of basement structures under east-west extension. Speed and Cogbill (1979) interpreted an east-west Candelaria trough in western Nevada that we now consider to be a paleovalley resulting from erosion and not from extension.

The other volcano-tectonic trough in Nevada proposed by Burke and McKee (1979) also has been shown to be a series of unrelated calderas spread across several mountain ranges (Fig. 1; McKee and Conrad, 1987; Hardyman et al., 1988; John, 1995). Lipman (1997) dismisses the existence of volcano-tectonic depressions in general, and most cited examples have been shown to be a series of partly overlapping calderas—for example, the Taupo volcanic zone in New Zealand (Wilson et al., 1984).

Relation to Nearby Carlin-Type Gold Deposits

Several Carlin-type gold deposits are adjacent to or within ~10 km of the Caetano caldera. The Cortez and Cortez Hills deposits lie ~5 and 2–3 km, respectively, from the northeastern edge of the caldera, Horse Canyon is ~4.5 km east of the caldera, and the Pipeline and Gold Acres deposits are ~7 km north of the caldera margin (Plate 1). Although Rytuba (1985) and Rytuba et al. (1986) proposed that Caetano magmatism provided the heat for mineralization at Cortez, mineralization at each of these deposits probably predates ash-flow eruption and caldera collapse, and Caetano Tuff in the northeastern part of the caldera is unaltered. However, caldera magmatism may have been the youngest manifestation of a sequence of genetically related igneous activity manifested by slightly older rhyolite dikes and domes exposed just outside the caldera.

At Cortez, porphyritic rhyolite dikes are hydrothermally altered but are variably interpreted as pre-, syn- or post-mineral (Wells et al., 1969, 1971; Rytuba et al., 1986; McCormack and Hays, 1996; R. Leonardson, 2007, oral commun). Mortensen et al. (2000) report a zircon U-Pb age of 35.2 ± 0.2 Ma for a dike from the Main pit at Cortez. If the dikes are post-mineral, then the caldera is ≥1.4 Ma younger than the gold mineralization. If the dikes are pre- or syn-mineral, then caldera activity may be much closer in time. Existing K-Ar ages (Wells et al., 1971) for other dikes (34.7 ± 1.1 to 35.8 ± 1.2 Ma) overlap K-Ar ages for nearby intracaldera Caetano Tuff (35.2 ± 1.1 (biotite) and 33.4 ± 1.0 Ma (sanidine)), and both are older than our $^{40}Ar/^{39}Ar$ ages for the Caetano Tuff (Table 1). Additional $^{40}Ar/^{39}Ar$ dating of the dikes is in progress and may help resolve these discrepancies.

Known igneous events around the nearby Carlin-type deposits are: (1) the Tenabo granite ~7 km northeast of Pipeline, which has a biotite $^{40}Ar/^{39}Ar$ age of 38.85 ± 0.07 Ma (Kelson et al., 2005); (2) the 35.2 Ma rhyolite dikes in the Cortez Mine and Cortez Range (Mortensen et al., 2000); (3) the tuff of Cove Mine at 34.2 Ma, although its source area is unknown and need not be nearby (this study); and (4) the Caetano caldera and intrusions at 33.8 Ma (this study). Many other igneous bodies are undated, and any genetic relationship between any of these and the gold deposits is speculative. The age of gold mineralization at Pipeline is interpreted to be 38.7 ± 2.0 Ma based on the average of seven out of 48 apatite fission-track ages (Arehart and Donelick, 2006). The data demonstrate that the Pipeline-Cortez area underwent significant magmatism over ca. 5 Ma between 39 and 33.8 Ma. The duration of magmatic activity in the Pipeline-Cortez area is similar to the 4 Ma period of igneous activity in the Carlin trend, between 40 and 36 Ma, during which time the world-class Carlin-type gold deposits formed (Hofstra et al., 1999; Henry and Ressel, 2000; Arehart et al., 2003; Ressel and Henry, 2006).

Reconstruction of the late Eocene, pre-Caetano caldera geologic setting also places constraints on the depth of formation of the Cortez Hills and Horse Canyon Carlin-type deposits (Plate 1). The presence of Paleozoic limestone clasts in conglomerates in the Wenban Spring area underlying the Caetano caldera floor and of limestone blocks in mesobreccia in intracaldera Caetano Tuff in the Toiyabe Range indicate that the Eocene paleovalley that extended west across the caldera from the Cortez Range had cut down into Paleozoic carbonate rocks of the lower plate of the Roberts Mountain allochthon prior to caldera formation. At the presumed Eocene time of mineralization, the paleovalley probably had only a thin gravel fill equivalent to the pre-volcanic gravel of the Caetano Ranch area. Upper parts of the gravel in the Cortez Range contain clasts of Caetano and Bates Mountain Tuffs; thus, it is much younger. The Cortez Hills deposit is hosted by lower plate Wenban Limestone west of the Cortez fault and, assuming the paleovalley trends nearly due west, lies ~1 km north of the northern edge of the paleovalley. Overlying upper plate rocks immediately east of the deposit and the Cortez fault are less than 1000 m thick (B–B', Plate 1; Gilluly and Masursky, 1965), which suggests that the top of the Cortez Hills deposit formed at no more than ~1000-m paleodepth. The Horse Canyon deposit occurs in upper plate rocks along the north side of the paleovalley east of the Cortez fault. This relationship suggests that the Horse Canyon deposit formed at very shallow depths, much less than 1 km.

ACKNOWLEDGMENTS

We greatly appreciate extensive discussions with Ted McKee, Sherman Grommé, Tom Moore, Alan Wallace, Bob Fleck, Zac Gonsior, John Dilles, Myron Best, Al Deino, and Bob Leonardson. Kerry Hart of Barrick Gold Corporation provided unpublished interpretations of the caldera margin in northern Grass Valley. $^{40}Ar/^{39}Ar$ dating was done at the New Mexico Geochronology Research Laboratory (New Mexico Institute of Mining and Technology) under the patient guidance of Bill McIntosh, Matt Heizler, Lisa Peters, and Rich Esser. Anita Harris examined two limestone samples for conodonts. Peter Lipman, Alexander Iriondo, Al Hofstra, and Sherman Grommé are thanked for their constructive reviews of an earlier version of this manuscript.

REFERENCES CITED

Arehart, G.B., and Donelick, R.A., 2006, Thermal and isotopic profiling of the Pipeline hydrothermal system: Application to exploration for Carlin-type gold deposits: Journal of Geochemical Exploration, v. 91, p. 27–40, doi: 10.1016/j.gexplo.2005.12.005.

Arehart, G.B., Chakurian, A.M., Tretbar, D.R., Christiansen, J.N., McInnes, B.A., and Donelick, R.A., 2003, Evaluation of radioisotope dating of Carlin-type deposits in the Great Basin, western North America, and implications for deposit genesis: Economic Geology and the Bulletin of the Society of Economic Geologists, v. 98, p. 235–248.

Bartley, J.M., 1989, Changing Tertiary extension direction in Dry Lake Valley, Nevada, and a possible dynamic model, *in* Garside, L.J., and Shaddrick, D.R., eds., Compressional and extensional structural styles in the northern Basin and Range Province–Seminar Proceedings: Reno, Nevada Petroleum Society and Geological Society of Nevada, p. 35–39.

Bartley, J.M., Taylor, W.J., and Lux, D.R., 1992, Blue Ribbon volcanic rift in southeastern Nevada and its effects on Basin and Range fault segmentation: Geological Society of America Abstracts with Programs, v. 24, no. 6, p. 2.

Best, M.G., 1988, Early Miocene change in direction of least principal stress, southwestern United States: Conflicting inferences from dikes and metamorphic core-detachment fault terranes: Tectonics, v. 7, p. 249–259.

Best, M.G., Christiansen, E.H., Deino, A.L., Grommé, C.S., McKee, E.H., and Noble, D.C., 1989, Excursion 3A: Eocene through Miocene volcanism in the Great Basin of the western United States: New Mexico Bureau of Mines and Mineral Resources Memoir, v. 47, p. 91–133.

Bingler, E.C., 1978, Abandonment of the name Hartford Hill Rhyolite Tuff and adoption of new formation names for middle Tertiary ash-flow tuffs in the Carson City-Silver City area, Nevada: U.S. Geological Survey Bulletin, 1457-D, 19 p.

Boden, D.R., 1986, Eruptive history and structural development of the Toquima caldera complex, central Nevada: Geological Society of America Bulletin, v. 97, p. 61–74, doi: 10.1130/0016-7606(1986)97<61:EHASDO>2.0.CO;2.

Boden, D.R., 1992, Geologic map of the Toquima caldera complex, central Nevada: Nevada Bureau of Mines and Geology Map 98, scale 1:48,000.

Brooks, E.R., Wood, M.M., Boehme, D.R., Potter, K.L., and Marcus, B.I., 2003, Geologic map of the Haskell Peak area, Sierra County, California: California Geological Survey Map Sheet 55.

Burke, D.B., and McKee, E.H., 1979, Mid-Cenozoic volcano-tectonic troughs in central Nevada: Geological Society

of America Bulletin, v. 90, no. Part 1, p. 181–184, doi: 10.1130/0016-7606(1979)90<181:MVTICN>2.0.CO;2.

Castor, S.B., Boden, D.R., Henry, C.D., Cline, J.S., Hofstra, A.H., McIntosh, W.C., Tosdal, R.M., and Wooden, J.P., 2003, Geology of the Eocene Tuscarora volcanic-hosted, epithermal precious metal district, Elko County, Nevada: Economic Geology and the Bulletin of the Society of Economic Geologists, v. 98, p. 339–366.

Christiansen, R.L., and Yeats, R.S., 1992, Post-Laramide geology of the U.S. Cordilleran region, *in* Burchfiel, B.C., Lipman, P.W., and Zoback, M.L., eds., The Cordilleran orogen; conterminous U.S.: Boulder, Colorado, Geological Society of America, the Geology of North America, v. G-3, p. 261–406.

Cline, J.S., Hofstra, A.H., Muntean, J.L., Tosdal, R.M., and Hickey, K.A., 2005, Carlin-type gold deposits in Nevada: Critical geologic characteristics and viable models: Economic Geology, One Hundredth Anniversary Volume, p. 451–484.

Colgan, J.P., John, D.A., and Henry, C.D., 2008, Large-magnitude Miocene extension of the Caetano caldera, southern Shoshone and northern Toiyabe Ranges: Geosphere, v. 4, no. 1, doi: 10.1130/GES00115.1.

Deino, A.L., 1989, Single crystal $^{40}Ar/^{39}Ar$ dating as an aid in correlation of ash flows: Examples from the Chimney Springs/New Pass Tuffs and the Nine Hill/Bates Mountain Tuffs of California and Nevada: New Mexico Bureau of Mines and Mineral Resources: Continental Magmatism Abstracts Bulletin, v. 131, p. 70.

Doebrich, J.L., 1995, Geology and mineral deposits of the Antler Peak 7.5-minute quadrangle, Lander County, Nevada: Nevada Bureau of Mines and Geology Bulletin 109, 44 p.

Emmons, D.L., and Eng, T.L., 1995, Geologic map of the McCoy mining district, Lander County, Nevada: Nevada Bureau of Mines and Geology Map 103, 12 p., 2 plates.

Faulds, J.E., Henry, C.D., and dePolo, C.M., 2003, Preliminary geologic map of the Tule Peak Quadrangle, Washoe County, Nevada: Nevada Bureau of Mines and Geology Open-File Report 03-10, 1:24,000.

Faulds, J.E., Henry, C.D., and Hinz, N.H., 2005, Kinematics of the northern Walker Lane: An incipient transform fault along the Pacific-North American plate boundary: Geology, v. 33, p. 505–508, doi: 10.1130/G21274.1.

Gilluly, J., 1977, Cauldron subsidence near Mount Lewis, Nevada—A misconception: U.S. Geological Survey Journal of Research, v. 5, p. 325–329.

Gilluly, J., and Gates, O., 1965, Tectonic and igneous geology of the northern Shoshone Range, Nevada, *with sections on* Gravity in Crescent Valley, by D. Plouff, *and* Economic geology, by K.B. Ketner: U.S. Geological Survey Professional Paper 465, 153 p.

Gilluly, J., and Masursky, H., 1965, Geology of the Cortez Quadrangle, Nevada: U.S. Geological Survey Bulletin 1175, 117 p.

Gonsior, Z.J., 2006, The timing and evolution of Cenozoic extensional normal faulting in the southern Tobin Range, Pershing County, Nevada: Nevada Bureau of Mines and Geology Open-File Report 06-4, 64 p.

Gonsior, Z.J., and Dilles, J.H., 2008, The timing and evolution of Cenozoic extensional normal faulting in the southern Tobin Range, Nevada: Geosphere (in press).

Grommé, C.S., McKee, E.H., and Blake, M.C., Jr., 1972, Paleomagnetic correlations and potassium-argon dating of middle Tertiary ash-flow sheets in the eastern Great Basin, Nevada and Utah: Geological Society of America Bulletin, v. 83, p. 1619–1638, doi: 10.1130/0016-7606(1972)83[1619:PCAPDO]2.0.CO;2.

Hardyman, R.F., Brooks, W.E., Blaskowki, M.J., Barton, H.N., Ponce, D.A., and Olson, J.E., 1988, Mineral resources of the Clan Alpine Wilderness Study Area, Churchill County, Nevada: U.S. Geological Survey Bulletin 1727-B, 16 p.

Henry, C.D., 2008, Ash-flow tuffs and paleovalleys in northeastern Nevada: Implications for Eocene paleogeography and extension in the Sevier hinterland, northern Great Basin: Geosphere, v. 4, no. 1, doi: 10.1130/GES00122.1.

Henry, C.D., and Ressel, M.W., 2000, Eocene magmatism of northeastern Nevada: The smoking gun for Carlin-type gold deposits, *in* Cluer, J.K., Price, J.G., Struhsacker, E.M., Hardyman, R.F., and Morris, C.L., eds., Geology and ore deposits 2000: The Great Basin and beyond: Geological Society of Nevada Symposium Proceedings, May 15–18, 2000, p. 365–388.

Henry, C.D., Elson, H.B., McIntosh, W.C., Heizler, M.T., and Castor, S.B., 1997, Brief duration of hydrothermal activity at Round Mountain, Nevada determined from $^{40}Ar/^{39}Ar$ geochronology: Economic Geology and the Bulletin of the Society of Economic Geologists, v. 92, p. 807–826.

Henry, C.D., Boden, D.R., and Castor, S.C., 1999, Geologic map of the Tuscarora Quadrangle, Nevada: Nevada Bureau of Mines and Geology Map 116, scale 1:24,000, 20 p. text.

Henry, C.D., Faulds, J.E., dePolo, C.M., and Davis, D.A., 2004, Geology of the Dogskin Mountain Quadrangle, northern Walker Lane, Nevada: Nevada Bureau of Mines and Geology Map 148, scale 1:24,000, 13 p. text.

Hess, R.H., and Johnson, G.L., 1997, County digital geological maps of Nevada: Nevada Bureau of Mines and Geology Open-File Report 97-1, (http://www.nbmg.unr.edu/dox/dox.htm)

Hofstra, A.H., Snee, L.W., Rye, R.O., Folger, H.W., Phinisey, J.D., Loranger, R.J., Dahl, A.R., Naesar, C.W., Stein, H.J., and Lewchuk, 1999, Age constraints on Jerritt Canyon and other Carlin-type gold deposits in the western United States—Relationship to mid-Tertiary extension and magmatism: Economic Geology and the Bulletin of the Society of Economic Geologists, v. 94, p. 769–802.

Hon, K., and Lipman, P.W., 1989, Western San Juan caldera complex, *in* Chapin, C.E., and Zidek, J., eds., Field excursions to the volcanic terranes in the western United States, volume 1: Southern Rocky Mountain region: New Mexico Bureau of Mines and Mineral Resources Memoir 46, p. 350–380

Irvine, T.N., and Baragar, W.R.A., 1971, A guide to the chemical classification of the common volcanic rocks: Canadian Journal of Earth Sciences, v. 8, p. 523–548.

Janecke, S.U., Hammond, B.F., Snee, L.W., and Geissman, J.W., 1997, Rapid extension in an Eocene volcanic arc: Structure and paleogeography of an intra-arc half graben in central Idaho: Geological Society of America Bulletin, v. 109, p. 253–267, doi: 10.1130/0016-7606(1997)109<0253:REIAEV>2.3.CO;2.

John, D.A., 1995, Tilted middle Tertiary ash-flow calderas and subjacent granitic plutons, southern Stillwater Range, Nevada: Cross sections of an Oligocene igneous center: Geological Society of America Bulletin, v. 107, no. 2, p. 180–200, doi: 10.1130/0016-7606(1995)107<0180:TMTAFC>2.3.CO;2.

John, D.A., and Pickthorn, W.J., 1996, Alteration and stable isotope studies of a deep meteoric-hydrothermal system in the Job Canyon caldera and IXL pluton, southern Stillwater Range, Nevada: *in* Coyner, A.R., and Fahey, P.L., eds., Geology and ore deposits of the American Cordillera: Reno/Sparks, Nevada, Geological Society of Nevada Symposium Proceedings, April 1995, p. 733–756.

John, D.A., and Wrucke, C.T., 2003, Geologic map of the Mule Canyon quadrangle, Lander County, Nevada: Nevada Bureau of Mines and Geology Map 144, scale 1:24,000, 16 p. (http://www.nbmg.unr.edu/dox.htm)

Kelson, C.R., Crowe, D., and Stein, H., 2005, Geochronology and geochemistry of the Hilltop, Lewis, and Bullion Mining Districts, Battle Mountain-Eureka trend, Nevada: Geological Society of America Abstracts with Programs, v. 37, no. 7, p. 314.

Le Bas, M.J., Le Maitre, R.W., Streckeisen, A., and Zanettin, B.A., 1989, Chemical classification of volcanic rocks based on the total alkali-silica diagram: Journal of Petrology, v. 27, p. 745–750.

Lipman, P.W., 1984, The roots of ash flow calderas in western North America: Windows into the tops of granitic batholiths: Journal of Geophysical Research, v. 89, p. 8801–8841.

Lipman, P.W., 1997, Subsidence of ash-flow calderas: Relation to caldera size and magma-chamber geometry: Bulletin of Volcanology, v. 59, p. 198–218, doi: 10.1007/s004450050186.

Lipman, P.W., 2000, The central San Juan caldera cluster: Regional volcanic framework, *in* Bethke, P.M., and Hay, R.L., eds., Ancient Lake Creede: Its volcano-tectonic setting, history of sedimentation, and relation of mineralization in the Creede Mining District: Geological Society of America Special Paper 346, p. 9–69.

Lipman, P.W., 2007, Incremental assembly and prolonged consolidation of Cordilleran magma chambers: Evidence from the southern Rocky Mountain volcanic field: Geosphere, v. 3, p. 42–70, doi: 10.1130/GES00061.1.

Lipman, P.W., Prostka, H.J., and Christiansen, R.L., 1972, Cenozoic volcanism and plate tectonic evolution of the western United States, I, Early and Middle Cenozoic: Philosophical Transactions of the Royal Society of London: Series A, v. 271, p. 217–248.

Ludington, S., Cox, D.P., Moring, B.C., and Leonard, K.W., 1996, Cenozoic volcanic geology of Nevada: Nevada Bureau of Mines and Geology Open-File Report 96-2, chapter 5, p. 5-1–5-10.

Masursky, H., 1960, Welded tuffs in the northern Toiyabe Range, Nevada: U.S. Geological Survey Professional Paper 400B, p. B281–283.

McCormack, J.K., and Hays, R.C., Jr., 1996, Crescent Valley: A model for reconstruction of district mineralization in the Basin and Range, *in* Coyner, A.R., and Fahey, P.L., eds., Geology and ore deposits of the American Cordillera: Reno/Sparks, Nevada, Geological Society of Nevada Symposium Proceedings, April, 1995, p. 635–646.

McIntosh, W.C., Heizler, M., Peters, L., and Esser, R., 2003, $^{40}Ar/^{39}Ar$ geochronology at the New Mexico Bureau of Geology and Mineral Resources: New Mexico Bureau of Geology and Mineral Resources Open-File Report OF-AR-1, 10 p.

McIntosh, W.C., Sutter, J.F., Chapin, C.E., and Kedzie, L.L., 1990, High-precision $^{40}Ar/^{39}Ar$ sanidine geochronology of ash-flow tuffs in the Mogollon-Datil volcanic field, southwestern New Mexico: Bulletin of Volcanology, v. 52, p. 584–601, doi: 10.1007/BF00301210.

McKee, E.H., 1968, Geologic map of the Spencer Hot Springs Quadrangle, Lander and Eureka Counties, Nevada: U.S. Geological Survey Geologic Quadrangle Map GQ-770.

McKee, E.H., 1970, Fish Creek Mountains Tuff and volcanic center, Lander County, Nevada: U.S. Geological Survey Professional Paper 681, 17 p.

McKee, E.H., and Conrad, J.E., 1987, Geologic map of the Desatoya Mountains Wilderness Study Area, Churchill and Lander counties, Nevada: U. S. Geological Survey Miscellaneous Field Studies Map MF-1944, scale 1:62,500.

McKee, E.H., and Conrad, J.E., 1994, Geologic map of the northern part of the Simpson Park Mountains, Eureka County, Nevada: U.S. Geological Survey Miscellaneous Field Studies Map MF-2257, scale 1:24,000.

McKee, E.H., and Moring, B.C., 1996, Cenozoic mineral deposits and Cenozoic igneous rocks of Nevada: Nevada Bureau of Mines and Geology Open-File Report 96-2, chapter 6, p. 6-1–6-8.

Moore, T.E., Murchey, B.L., and Harris, A.G., 2000, Significance of geologic and biostratigraphic relations between the Overlap assemblage and Havallah sequence, southern Shoshone Range, Nevada, *in* Cluer, J.K., Price, J.G., Struhsacker, E.M., Hardyman, R.F., and Morris, C.L., eds., Geology and ore deposits 2000: The Great Basin and beyond: Geological Society of Nevada Symposium Proceedings, May 15–18, p. 397–418.

Mortensen, J.K., Thompson, J.F.H., and Tosdal, R.M., 2000, U-Pb age constraints on magmatism and mineralization in the northern Great Basin, Nevada, *in* Cluer, J.K., Price, J.G., Struhsacker, E.M., Hardyman, R.F., and Morris, C.L., eds., Geology and ore deposits 2000: The Great Basin and beyond: Geological Society of Nevada Symposium Proceedings, May 15–18, p. 419–438.

Newhall, C.G., and Dzurisin, D., 1988, Historical unrest at large calderas of the world: U.S. Geological Survey Bulletin 1855, 597 p.

Nutt, C.J., 2000, Geologic map of the Alligator Ridge area, including the Buck Mountain East and Mooney Basin Summit quadrangles and parts of the Sunshine Well NE and Long Valley Slough quadrangles, White Pine County, Nevada: U.S. Geological Survey Geologic Investigations Series I-2691, scale 1:24,000.

Price, J.G., and Meeuwig, R.O., 2006, Overview: The Nevada mining industry 2005: Nevada Bureau of Mines and Geology Special Publication, v. MI-2005, p. 3–12.

Renne, P.R., Swisher, C.C., Deino, A.L., Karner, D.B., Owens, T.L., and DePaolo, D.J., 1998, Intercalibration

of standards, absolute ages and uncertainties in $^{40}Ar/^{39}Ar$ dating: Chemical Geology, v. 145, p. 117–152, doi: 10.1016/S0009-2541(97)00159-9.

Ressel, M.W., and Henry, C.D., 2006, Igneous geology of the Carlin trend, Nevada: Development of the Eocene plutonic complex and significance for Carlin-type gold deposits: Economic Geology and the Bulletin of the Society of Economic Geologists, v. 101, p. 347–383.

Roberts, R.J., 1964, Stratigraphy and structure of the Antler Peak quadrangle, Humboldt and Lander Counties, Nevada: U.S. Geological Survey Professional Paper 459-A, 93 p.

Roberts, R.J., Hotz, P.E., Gilluly, J., and Ferguson, H.G., 1958, Paleozoic rocks of north-central Nevada: American Association of Petroleum Geologists Bulletin, v. 42, p. 2813–2857.

Rowley, P.D., 1998, Cenozoic transverse zones and igneous belts in the Great Basin, western United States: Their tectonic and economic implications, *in* Faulds, J.E., and Stewart, J.H., eds., Accommodation zones and transfer zones: The regional segmentation of the Basin and Range province: Geological Society of America Special Paper 323, p. 195–228.

Rytuba, J.J., 1985, Development of disseminated gold deposits of Cortez, Horse Canyon, and Gold Acres, Nevada, at the end stage of caldera-related volcanism: U.S. Geological Survey Circular 949, p. 47.

Rytuba, J.J., Madrid, R.J., and McKee, E.H., 1986, Relationship of the Cortez caldera to the Cortez disseminated gold deposit, Nevada: Journal of Geochemical Exploration, v. 25, p. 251, doi: 10.1016/0375-6742(86)90046-4.

Samson, S.D., and Alexander, E.C., Jr., 1987, Calibration of the interlaboratory $^{40}Ar/^{39}Ar$ dating standard, MMhb-1: Chemical Geology, v. 66, p. 27–34.

Sargent, K.A., and McKee, E.H., 1969, The Bates Mountain Tuff in northern Nye County, Nevada: U.S. Geological Survey Bulletin, v. 1294-E, 12 p.

Sloan, J., Henry, C.D., Hopkins, M., and Ludington, S., 2003, Revision of National Geochronological Database: U.S. Geological Survey Open-File Report 03-236, http://wrgis.wr.usgs.gov/open-file/of03-236/.

Smith, R.L., and Bailey, R.A., 1968, Resurgent cauldrons: Geological Society of America Memoir 116, p. 613–662.

Speed, R.C., and Cogbill, A.H., 1979, Deep fault trough of Oligocene age, Candelaria Hills, Nevada: Geological Society of America Bulletin, v. 90, no. part 1, p. 145–148, doi: 10.1130/0016-7606(1979)90<145:DFTOOA>2.0.CO;2.

Steiger, R.H., and Jäger, E., 1977, Subcommission on geochronology: Convention on the use of decay constants in geo- and cosmochronology: Earth and Planetary Science Letters, v. 36, p. 359–362, doi: 10.1016/0012-821X(77)90060-7.

Stewart, J.H., and Carlson, J.E., 1976, Geologic map of north-central Nevada: Nevada Bureau of Mines and Geology Map 50, scale 1:250,000.

Stewart, J.H., and McKee, E.H., 1968, Geologic map of the Mount Callaghan Quadrangle, Lander County, Nevada: U.S. Geological Survey Geologic Quadrangle Map GQ-730, 1:62,500.

Stewart, J.H., and McKee, E.H., 1977, Geology and mineral deposits of Lander County, Nevada: Part 1—Geology: Nevada Bureau Of Mines and Geology Bulletin 88, 59 p.

Wells, J.D., Elliott, J.E., and Obradovich, J.D., 1971, Age of the igneous rocks associated with ore deposits, Cortez-Buckhorn area, Nevada: U.S. Geological Survey Professional Paper 750-C, p. C127–C135.

Wells, J.D., Stoiser, L.R., and Elliot, J.E., 1969, Geology and geochemistry of the Cortez gold deposit: Economic Geology and the Bulletin of the Society of Economic Geologists, v. 64, p. 526–537.

Wilson, C.J.N., Rogan, A.M., Smith, I.E.M., Northey, D.J., Nairn, I.A., and Houghton, B.F., 1984, Caldera volcanoes of the Taupo volcanic zone, New Zealand: Journal of Geophysical Research, v. 89, p. 8436–8484.

Wrucke, C.T., and Silberman, M.L., 1975, Cauldron subsidence of Oligocene age at Mount Lewis, northern Shoshone Range, Nevada: U.S. Geological Survey Professional Paper 876, 19 p.

Wrucke, C.T., and Silberman, M.L., 1977, Cauldron subsidence of Oligocene age at Mount Lewis, Shoshone Range, Nevada—A reasonable interpretation: U.S: Geological Survey Journal of Research, v. 5, p. 331–335.

Manuscript Received 30 March 2007
Revised Manuscript Received 20 August 2007
Manuscript Accepted 25 August 2007